Decarbonizing Regional Multi-Modal Transportation System with Shared Electric Charging Hub

Zuzhao Ye, Nanpeng Yu
Department of Electrical and Computer Engineering
University of California, Riverside
Riverside, CA, USA
zye066@ucr.edu, nyu@ece.ucr.edu

Ran Wei
School of Public Policy
University of California, Riverside
Riverside, CA, USA
ran.wei@ucr.edu

Xiaoyue Cathy Liu
Department of Civil and Environmental Engineering
University of Utah
Salt Lake City, UT, USA
cathy.liu@utah.edu

Abstract

In light of the growing concerns of global climate change, the pace of transportation electrification has greatly accelerated in recent years as an effort towards net-zero greenhouse gas (GHG) emissions. However, it remains unclear how to effectively deploy and operate public charging infrastructure to best serve an electrified transportation system within a multi-modal context while maximizing the benefits of decarbonization. This is especially true when considering the GHG emitted by generating one kWh of electricity, i.e. the electricity carbon intensity, varies across a day due the change of generation mix between renewable and fossil fueled resources. To address this question, we propose a mechanism of shared charging hubs that can provide holistic energy management for both electric buses (EBs) and passenger electric vehicles (EVs).The deployment and operation of shared charging hubs is determined by a new spatio-temporal optimization model which aims to minimize GHG emission given a budget limit while avoiding the occurrence of massive spikes in peak power demand. This is achieved by coherently accommodating the charging demand of EBs and EVs, and explicitly integrating the time-varying electricity carbon intensity and vehicle-to-grid (V2G) technology. To demonstrate its effectiveness, the model is applied to the bus fleets operated by seven transit agencies and the park-and-ride facilities (for EVs) near twelve rail transit stations in Contra Costa County, California, USA. The results show that the shared charging hubs can lead to significant GHG emission reduction while mitigating the peak electricity demand. This research will help policymakers and transportation agencies make more informed decisions regarding the planning and design of charging infrastructure.

Keywords Decarbonization · Shared charging hub · Electricity carbon intensity · V2G

1 Introduction

Achieving net-zero global greenhouse gas (GHG) emissions by the mid of this century is essential to reaching the well-below 2°C and 1.5°C objectives of the Paris Agreement [Obergassel et al., 2016]. Transport sector produces more than 16% of the global GHG emissions measured in CO_2 equivalent (CO_2e). In the US, France and several other developed countries, the transport sector accounts for around a third of the overall GHG emissions, and its pace of growth is the fastest among all economic sectors [Ritchie and Roser, 2020]. Hence, proper analysis and planning to decarbonize the transport sector is critical to fight against climate change. Transportation electrification is well-recognized as a key pathway towards this goal [Lutsey and Sperling, 2009, Pan et al., 2018, Sofia et al., 2020].

There are a variety of transportation modes in the modern multimodal transportation system, all of which are quickly embracing electrification. For example, the sales of passenger electric vehicles (EVs) in 2021 increased by 168% and 104% in China [CAAM, 2022] and the US [Gohlke and Zhou, 2021, Zhou, 2022], respectively, compared with the previous year. In some European countries EVs are drastically taking over the market. For example, EVs made up more than 80% of Norway's new sales in 2021[Kane, 2022]. In the public transport sector, the adoption of electric buses (EBs) started in China, and its pace is now accelerating worldwide [Sustainable-Bus, 2020]. In Western Europe, the number of new EB registrations was 2,062 in 2020, while this number was only 562 in 2018 [Sustainable-Bus, 2018]. In the US, the EB deployment has grown by 24% in 2021, reaching 3,364 EBs [CALSTART, 2021]. The fast expansion of EB fleets in the near future is foreseeable. Recently in California, the state regulation requires that beginning in 2029, 100% of new purchases made by transit agencies must be zero-emission buses, with a goal for full transition by 2040 [CARB, 2019]. The growing popularity of electrified transportation requires a similar scale-up of the charging infrastructure. While many countries have been making significant investment in the deployment of charging infrastructure, they separate different modes (e.g., EV and EB) in their designs and planning, rather than jointly considering them together. Given the ever-increasing interactions among these electrified transportation modes, it is essential to holistically integrate all of these modes into the strategic planning and design of the charging infrastructure to produce an efficient and low-carbon electrified transportation ecosystem.

In this paper we propose that policy makers deploy shared charging hubs to provide integrative energy management for two of the most important electrified transportation modes, EVs and EBs. There are quite a few unique benefits associated with such shared charging hubs. First of all, the EB chargers and EV chargers can share common power equipment, e.g. distribution wires, converters, inverters, and sub-stations. Such a sharing scheme produces an economy of scale and makes the charging hub a potentially more cost-effective option compared to charging stations dedicated to a single mode. Secondly, the peak power demand can be mitigated through coordinated operations of EBs and EVs, which further reduces the immediate power capacity investment as well as the long-term electricity bills. Thirdly, the shared charging hubs can bridge different transportation modes. An important factor that hinders the usage of public transportation is the lack of connections between communities and transit facilities, also known as the first-and-last mile issue [Zuo et al., 2020]. Especially in the US, a dispersed land-use pattern is predominant outside urbanized regions and the use of fixed-route transit systems is implicitly discouraged [Lesh, 2013]. Such a situation could be improved by establishing a charging hub close to the transit stations. The ridership of transit will be potentially boosted through attracting EV owners to park, charge, and finally travel with the public transportation system. Similar effects can be found with riders of e-scooters and e-bikes.

This article is outlined as follows: Section 2 provides a comprehensive review of the literature. Section 3 highlights the contributions of this article. Section 4 formulates the overall optimization framework, including the objectives and the necessary constraints and assumptions. Section 5 introduces the selected study area and how the required input data are obtained and processed. Section 6 presents the optimization results and analyzes their impacts and implications. Finally, conclusions and suggestions for future research are presented in Section 7.

2 Literature Review

2.1 Charging Infrastructure Planning

There are many inspiring works regarding charging infrastructure planning in the existing literature. Most of the studies attempted to determine where charging stations should be located and how many chargers should be installed. Early pioneering work focused on EVs. [Frade et al., 2011] introduced a maximal coverage model to serve the node-based EV demand. [Jung et al., 2014] presented a bi-level programming method to locate charging stations for electric taxis through dynamically bridging the gap between global optimal and user equilibrium solutions of time cost minimization. [Zhang et al., 2017] connected the charging demand with traffic flow to capture its time-varying characteristic and formulated a capacitated flow refueling location model to handle the planning problem. Considering the locations of charging stations can impact the route choice of EV users, which further affects the traffic flow pattern, [Ghamami et al., 2020] developed an integrated model to determine routes and locations simultaneously. The utilization of real-world vehicle GPS data improved the estimation of charging demand, and resulted in a more informative planning [Yang et al., 2017, Kontou et al., 2019]. Range anxiety is a well-known obstacle to the adoption of EVs and in order to reduce it, [Kavianipour et al., 2021] proposed to model the charging behaviors in detail when planning the charging infrastructure. While the aforementioned model-based methods analyze the system from a top-down point of view, agent-based methods start from modeling micro-scale user behaviors and obtain the macro-scale characteristics through interactions between EVs, candidate charging stations, and road networks. Related work can be found in [Sweda and Klabjan, 2011, Sheppard et al., 2016, Pagani et al., 2019, Wolbertus et al., 2021].

In contrast to EVs, for which the charging demand can be generally approximated via stochastic modeling or derived from traffic data, EBs have exact and rigid operational schedules. In addition, the cost of converting one conventional bus (using either diesel or compressed natural gas as fuel) to an EB is substantial and this cost needs to be considered as most transit agencies rely on public funding. Therefore, the deployment of charging infrastructure for EBs requires careful planning to ensure that the energy demand of each individual bus is satisfied. Terminal charging is the most common assumption made in the existing literature. Under this assumption, [Kunith et al., 2017] simultaneously determined the minimum number and location of required charging stations for a bus network as well as the adequate battery capacity for each bus line by solving a capacitated set-covering problem. [Wei et al., 2018] developed a spatio-temporal optimization model to identify which bus in a fleet can be electrified and where charging stations should be built while the overall cost is minimized. Targeting a fully electrified fleet, [Stumpe et al., 2021] conducted a joint optimization to determine both charging infrastructure locations and vehicle schedules, and analyzed the sensitivity of location decision to the system parameters. In addition to terminal charging, battery swapping stations [Moon et al., 2020] and charging lanes [Liu et al., 2017] have also been investigated for applications in EBs. The cost competitiveness of different types of charging infrastructure was analyzed by [Chen et al., 2018].

Multistage deployment is another interesting aspect of charging infrastructure planning. In addition to where and how much investment should be made, literature in this direction strives to answer the question of when to invest, with the objectives of meeting the growing charging demand and reducing idling of resources [Xie et al., 2018, Lin et al., 2019].

In summary, while numerous research efforts have been dedicated to the planning of charging infrastructure, they are either solely focused on EBs or EVs. The shared charging hub concept for both vehicle types is rarely mentioned.

2.2 Time-varying Electricity Carbon Intensity

It must be recognized that electrification alone only reduces the GHG emissions of the transport sector, at the cost of increasing the emissions of the upstream power generation. The rate of GHG emission from power generation is usually termed as electricity carbon intensity (ECI) and measured by gCO_2e/kWh. The ECI can vary significantly from time to time, depending on the real-time generation mix. In areas with high penetration of solar generation, the ECI is usually low at noon and high after sunset. For example, on a specific day (Oct 21, 2021) in California, the lowest and highest ECIs are 222 and 374 gCO_2e/kWh, found at around 11 AM and 9 PM, respectively [CAISO, 2021]. A study of the Great Britain grid indicates the range of ECI can be as large as 79 to 447 gCO_2e/kWh [Dixon et al., 2020]. The time-varying ECI implies an opportunity to reduce GHG emissions through demand-side management. [Hoehne and Chester, 2016, Brinkel et al., 2020] proposed to schedule the charging sequences of EVs based on the real-time ECI of the grid such that the EVs' carbon footprint is minimized. On the other hand, the charging of EVs can also be coordinated to absorb excess wind generation to lower the effective grid ECI [Dixon et al., 2020]. Increasing the number of chargers for ECI-oriented scheduling [Tu et al., 2020] and incentivizing consumer charging behavior to use less carbon-intense electricity [Santarromana et al., 2020] can also greatly reduce the overall GHG emissions. All of these studies show great potential for considering time-varying ECI in charging scheduling. While in the past, electricity price was the most commonly used signal to shift charging demands, ECI is expected to be a new type of signal, especially in recent years as containing GHG emissions is becoming more urgent in global affairs and carbon trade has been adopted by more and more districts. However, most of the existing planning studies of charging infrastructure use either first-come-first-serve or cost-oriented charging schedules. It remains largely unclear how ECI-oriented smart charging scheduling can impact the planning outcome.

2.3 Vehicle-to-Grid

Another aspect worth noting is that the vehicle-to-grid (V2G) setting is rarely considered in the existing charging infrastructure planning studies, whose major goals are to satisfy the charging demand or to maximize the total energy-charged. Sending electricity back to the grid through the V2G function is likely to contradict these objectives. However, for a large portion of charging events, EVs are connected to charger outlets much longer than the necessary time to meet their charging needs [Sadeghianpourhamami et al., 2018, Gerritsma et al., 2019]. Under this scenario, owners of individual vehicles or charging infrastructure might be willing to inversely trade energy with the grid if they are incentivized. The applications of V2G in energy arbitrage, load shifting, frequency regulation, and other power system regulation services are covered by a great number of studies [Sarker et al., 2016, López et al., 2015, Pillai and Bak-Jensen, 2010]. Similar ideas can be extended to reducing GHG emissions by shifting the triggering signal from electricity prices or grid requests to time-varying ECI. It is important to examine whether and how the V2G could contribute to the reduction of GHG emissions in the planning and operation of charging infrastructure.

3 Contribution

To fill the gaps in the literature and provide necessary information to the policymakers, this paper proposes a mechanism for the planning of shared charging hubs for the two most prevailing transportation modes: EBs and EVs. The primary objective of the planning model is to minimize the GHG emissions in a regional area under a given annual budget, considering smart charging scheduling enabled by the awareness of time-varying ECI and the application of V2G technology. The output of the planning framework consists of decisions on the deployment of charging infrastructure, the electrification of existing conventional buses, as well as the optimized charging schedules. The contributions of this paper are highlighted as follows:

1) A scheme of shared charging hubs is proposed to serve the charging demand of multiple transportation modes. To the best of our knowledge, most charging infrastructure planning studies have focused on a single transportation mode, but a shared scheme between multiple modes is rarely examined. To address this gap, this paper studies the shared charging hubs for EBs and EVs as an illustration and analyzes the benefit of reducing required power capacity through coordinated charging. In addition to EBs and EVs, this framework can be easily extended to other electric transportation modes, such as e-bikes and e-scooters, to form a comprehensive multi-modal ecosystem of electrified mobilities.

2) The proposed framework pays special attention to the time-varying ECI and V2G technology. Currently, the impacts of time-varying ECI and V2G are mostly analyzed in the charging scheduling algorithms, but how they could influence the upstream deployment of charging infrastructure remains largely unexplored. This paper analyzes the potential of decarbonization through integrating ECI-oriented charging scheduling and V2G technology in the planning phase and identifies the optimal resource allocation under these settings to minimize GHG emissions.

4 Model Formulation

4.1 Problem Description

In a regional area, suppose there are a set I of public conventional buses and a set J of private EVs. The goal of local public decision-makers is to minimize the GHG emissions from buses and EVs sectors through the following strategies: 1) converting the conventional buses to EBs, 2) providing charging services to both EBs and EVs in a set K of candidate charging hubs, and 3) optimize the charging schedules of EBs and EVs according to the time-varying ECI. Note that converting non-electric private vehicles to EVs is relying on the decisions of individuals and it is hence not within the scope of this study. The deployment of these strategies is subject to constraints of operational schedule of buses, energy limits of EBs and EVs, number of installed EB/EV chargers, number and power capacities of the deployed charging hubs, and most importantly, the budget. Table 1 lists the notations used in this study. The following assumptions are made in the proposed model:

- The public transit agencies will be leasing charging infrastructure and EBs from private vendors on an annual basis to reduce the financial risk of high upfront costs and the costs associated with large fleet maintenance, as proposed in [Electrification Coalition, 2010, Li et al., 2018, Jattin, 2019] and practiced by [Lunden, 2018, Proterra, 2022].
- EBs can be charged in a charging hub or its depot and EVs can be charged in a charging hub or at home. For the EBs/EVs to be charged in a charging hub, there need to be sufficient EB/EV chargers. On the other hand, it is assumed that the charging facilities in bus depots are ready for use as buses are congregated in depots and charging infrastructure can be established in an economically efficient way by corresponding transit agencies. It is also assumed EVs have access to low-power chargers at home, which does not rely on the budget of public transit agencies.
- An EB can be charged in a charging hub if the following two conditions are satisfied: The EB's terminal station(s) is within a certain threshold distance (e.g. 0.5 mile) of a charging hub and its dwell time in the terminal is longer than a threshold time (e.g. 10 minutes). Given the first condition, the energy consumption and time to drive EBs to/from the charging hub can be neglected. For example, in Figure 1, a bus dwelling at terminal T1 will have access to Charging Hub 1 if d is less than 0.5 mile and its dwelling time is more than 10 minutes. Being close to a stop rather than a terminal does not qualify a charging hub to be used by an EB, as a bus usually has very limited dwell time at a stop. Binary parameters β_{ikt} are used to indicate if bus i at time t is having access to candidate charging hub k.
- An EV can be charged in a charging hub when it is parked in a charging hub. Binary parameters γ_{jkt} are used to indicate if EV j at time t is parked at the location of candidate charging hub k. The EV chargers can be shared among EVs through a smart charging scheme such that when one EV's charging demand is satisfied,

the charger can be moved to other waiting EVs, reducing the cost of leasing extra chargers. Such a scheme can be achieved through multiple ways, e.g. mobile chargers [Doll, 2022].

- The schedules of individual buses are kept unchanged after they are converted to EBs, relieving the potential frictions in transit agencies during the transition phase. The schedules of individual buses are known parameters. For bus i, $T_i^{departure}$, T_i^{depot}, and $T_i^{b,hub}$ are the sets of time steps for departure from a terminal, being in the depot, and having access to a candidate charging hub, respectively. It is worth noting that $T_i^{b,hub} = \{t \in T | \sum_{k \in K} \beta_{ikt} > 0\}$.
- The behavior of EVs will be derived from certain surveys and is assumed to be known parameters. $T_j^{v,hub}$ and T_j^{home} are the sets of time steps at which EV j is parked in a charging hub and parked at home, respectively.

The above assumptions are made to greatly enhance the flexibility of charging. It can help obtain an optimistic estimation of decarbonization potential that can serve as a baseline and reference for future policy decisions.

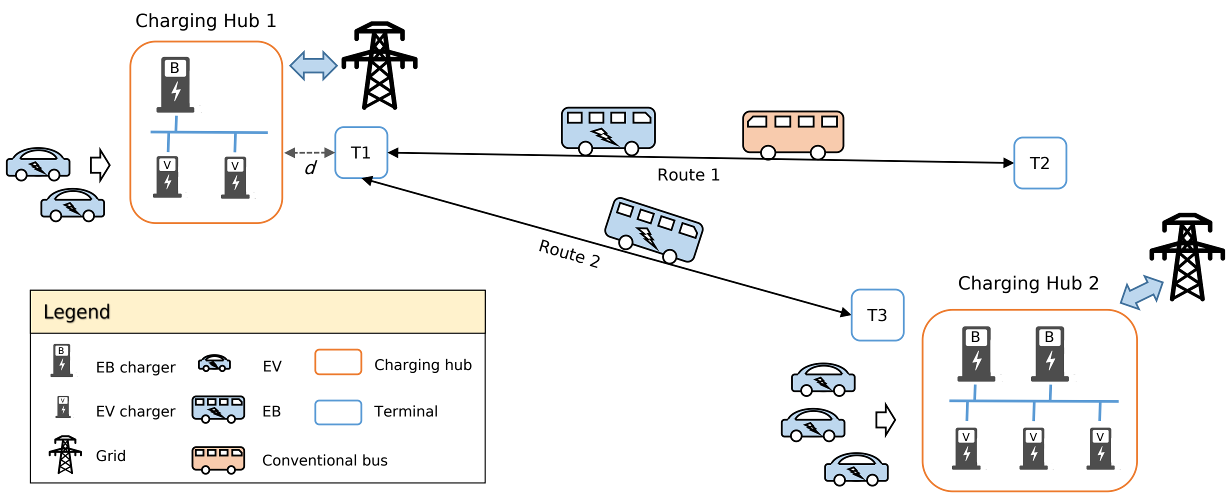

Figure 1: Illustration of the proposed problem.

4.2 Objective Function

The objective function is the minimization of the sum of GHG emissions from the bus and the EV sectors:

$$\min U^b + U^v, \tag{1}$$

where U^b and U^v are the GHG emissions from the bus sector and EV sector respectively, and:

$$U^b = \sum_{i \in I}(1 - z_i)u_i^b + \sum_{i \in I}\sum_{t \in T} g_t x_{it} \Delta t, \tag{2}$$

$$U^v = \sum_{j \in J}\sum_{t \in T} g_t y_{jt} \Delta t, \tag{3}$$

For the bus sector, U^b is jointly determined by conventional buses and EBs. The GHG emission from conventional buses is measured by $\sum_{i \in I}(1 - z_i)u_i^b$ where u_i^b is the daily GHG emission from bus i when it is a conventional bus. $z_i = 1$ indicates that bus i is converted to an EB such that its GHG emission from consuming fossil fuels is removed. On the other hand, despite zero on-road emission, EBs still create GHG emissions on the upstream power generation. The amount of GHG emissions from EBs is measured by $\sum_{i \in I}\sum_{t \in T} g_t x_{it} \Delta t$, where g_t is the ECI at time t and x_{it} is the charging power on bus i at time t. Δt is the length of time corresponding to one time step. For the EV sector, U^v is solely determined by EVs and it is measured by $\sum_{j \in J}\sum_{t \in T} g_t y_{jt} \Delta t$, where y_{jt} is the charging power on EV j at time t.

Table 1: Summary of notations for sets, parameters, and decision variables.

	Sets
I	Set of buses.
J	Set of EVs.
K	Set of candidate charging hubs.
T	Set of time steps of the study time horizon.
$T_i^{departure}$	Set of time steps at which bus i departs from its terminal stations.
T_i^{depot}	Set of time steps at which bus i is parking in its depot.
$T_i^{b,hub}$	Set of time steps at which bus i is having access to a candidate charging hub.
$T_j^{v,hub}$	Set of time steps at which EV j is parking in a candidate charging hub.
T_j^{home}	Set of time steps at which EV j is parking at home.
	Parameters
u_i^b	Daily carbon emission of bus i if it uses diesel as the fuel.
g_t	Electricity carbon intensity of the grid at time t.
$e^{b,min}/e^{b,max}$	Minimal/maximal battery energy of an EB.
$e^{v,min}/e^{v,max}$	Minimal/maximal battery energy of an EV.
x^{min}/x^{max}	Minimal/maximal charging powers of a bus charger.
y^{min}/y^{max}	Minimal/maximal charging powers of an EV charger.
$y^{home,min}/y^{home,max}$	Minimal/maximal charging powers of an EV home charger.
s_{it}^b	Power consumption rate of bus i at time t.
s_{jt}^v	Power consumption rate of EV j at time t.
η_b	Energy efficiency of EBs.
η_v	Energy efficiency of EVs.
κ	Cycle efficiency of charging/discharging batteries.
d_i	One-way distance of the route served by bus i.
β_{ikt}	$\beta_{ikt} = 1$ indicates bus i has access to candidate charging hub k at time t. Otherwise, $\beta_{ikt} = 0$.
γ_{jkt}	$\gamma_{jkt} = 1$ indicates EV j is parking in candidate charging hub k at time t. Otherwise, $\gamma_{jkt} = 0$.
c^b	Cost of one EB charger.
c^v	Cost of one EV charger.
c^p	Cost of providing one kW of power capacity at a charging hub.
c^f	Cost of make-ready, including licensing, construction, and etc.
c^{eb}	Cost of one EB.
c_t^e	Cost of charging 1kWh electricity at time t in a charging hub (commercial rate).
$c_t^{e,home}$	Cost of charging 1kWh electricity at time t at home (residential rate).
c^{deg}	Cost of battery degradation by charging/discharging 1kWh of electricity.
B	Budget.
	Decision Variables
U^b	Daily GHG emission of the bus sector.
U^v	Daily GHG emission of the EV sector.
z_i	Binary variable, $z_i = 1$ indicates bus i is electrified. Otherwise, $z_i = 0$.
x_{it}	Charging power on bus i at time t.
y_{jt}	Charging power on EV j at time t.
P_k^{cap}	Power capacity of charging hub k.
P_{kt}^b	Power demand of EBs in charging hub k at time t.
P_{kt}^v	Power demand of EVs in charging hub k at time t.
N_k^b	Number of EB chargers installed at charging hub k.
N_k^v	Number of EV chargers installed at charging hub k.
n_{kt}^b	Number of EBs charging in hub k at time t.
n_{kt}^v	Number of EVs charging in hub k at time t.
$\hat{N}_k$	$\hat{N}_k = 1$ indicates the candidate charging hub k is deployed. Otherwise, $\hat{N}_k = 0$.

4.3 Constraints

4.3.1 Bus Sector

$$e^b_{it'} = e^b_{it} + \left[x_{it} - (1-\sqrt{\kappa})|x_{it}| - z_i s^b_{it}\right]\Delta t, \quad \forall i \in I, \forall t \in T, t' = Next(t) \tag{4}$$

$$e^b_{it} \geq \frac{d_i}{\eta^b} - (1-z_i)G, \quad \forall i \in I, \forall t \in T_i^{departure}, \tag{5}$$

$$z_i e^{b,min} \leq e^b_{it} \leq z_i e^{b,max}, \quad \forall i \in I, \forall t \in T, \tag{6}$$

$$z_i x^{min} \leq x_{it} \leq z_i x^{max}, \quad \forall i \in I, \forall t \in \{T_i^{b,hub} \cup T_i^{depot}\}, \tag{7}$$

$$x_{it} = 0, \quad \forall i \in I, \forall t \notin \{T_i^{b,hub} \cup T_i^{depot}\}, \tag{8}$$

$$z_i \in \{0,1\}, \quad \forall i \in I, \tag{9}$$

Constraint (4) defines the transition rule of the battery energy level of the bus i from time t to the next time step t'. The $Next(\cdot)$ function is defined as follows: If t is the last time step of the day, $Next(t)$ will be the first time step of the day. Otherwise, $Next(t) = t + \Delta t$. Under such arrangement, the energy level of a bus will form a repeated closed-loop, which guarantees sustained inter-day operation. The energy loss due to charging/discharging is considered and measured by $-(1-\sqrt{\kappa})|x_{it}|$ (refer to [Foggo and Yu, 2017]), where κ is the battery cycle efficiency. s^b_{it} is the power consumption rate of bus i at time t. Constraint (5) requires that a bus needs to have enough energy to cover an entire trip upon departure, where d_i is the one-way distance of the route served by bus i and η^b is the electricity fuel efficiency of EBs. G is a relatively large positive number such that constraint (5) is only binding for EBs but not for conventional buses. Constraint (6) specifies the range of bus energy level, while constraint (7) specifies the range of bus charging power. When $x^{min} < 0$, the EBs are allowed to be discharged and send energy back to the grid. Note that when a bus is not in a charging hub or its depot, its charging power is zero as stated in constraint (8).

Constraints (4)-(9) are simultaneously applicable to conventional buses and EBs. When bus i is a conventional bus, i.e. $z_i = 0$, constraints (4), (5), (6), (7), and (8) are satisfied automatically with $e^b_{it} = 0, x_{it} = 0, \forall i \in I, t \in T$. This also means that there is no energy or power constraint for conventional buses, considering the fact that conventional buses can easily obtain fuel supply from existing fossil fuel infrastructure.

4.3.2 EV Sector

$$e^v_{jt'} = e^v_{jt} + \left[y_{jt} - (1-\sqrt{\kappa})|y_{jt}| - s^v_{jt}\right]\Delta t, \quad \forall j \in J, \forall t \in T, t' = Next(t) \tag{10}$$

$$e^{v,min} \leq e^v_{jt} \leq e^{v,max}, \quad \forall j \in J, \forall t \in T, \tag{11}$$

$$y^{min} \leq y_{jt} \leq y^{max}, \quad \forall j \in J, \forall t \in T_j^{v,hub}, \tag{12}$$

$$y^{home,min} \leq y_{jt} \leq y^{home,max}, \quad \forall j \in J, \forall t \in T_j^{home}, \tag{13}$$

$$y_{jt} = 0, \quad \forall j \in J, \forall t \notin \{T_j^{v,hub} \cup T_j^{home}\} \tag{14}$$

Constraint (10) defines the transition rule of the battery energy level of EV j from time t to the next time step t'. Similar to EBs, the energy loss due to charging/discharging is measured by $-(1-\sqrt{\kappa})|y_{jt}|$. s^v_{jt} is the power consumption rate of EV j at time t. While EBs need to have sufficient energy upon every departure, EVs are more flexible. Hence, it is assumed that the only requirement is that the daily amount of electricity charged into an EV is equal to their daily energy consumption, such that they can maintain sustained operation, as implied by (10). Constraint (11) specifies the range of an EV's battery energy level. Constraints (12) and (13) determine the range of EV charging power in a charging hub and at home. Specifying different charging power limits in different places is due to the fact that home charging is usually under alternating current and lower charging powers. Constraint (14) mandates that when an EV is not in a charging hub or at home, its charging power is zero.

4.3.3 Power Capacity

$$P_k^{cap} \geq |P_{kt}^b + P_{kt}^v|, \quad \forall k \in K, \forall t \in T, \tag{15}$$

$$P_{kt}^b = \sum_{i \in I} \beta_{ikt} x_{it}, \quad \forall k \in K, \forall t \in T, \tag{16}$$

$$P_{kt}^v = \sum_{j \in J} \gamma_{jkt} y_{jt}, \quad \forall k \in K, \forall t \in T, \tag{17}$$

There must be enough power capacity P_k^{cap} in each charging hub k to fulfill the combined peak charging power of EBs and EVs at any time t, as shown in constraint (15). The charging power of EBs P_{kt}^b or EVs P_{kt}^v at a charging hub k at time t is the sum of the charging power of individual EBs/EVs that are dwelling at the charging hub k at the time, indicated by binary parameters β_{ikt} for EBs, or γ_{jkt} for EVs. The use of the absolute sign in the right-hand side of constraint (15) considers the potential negative charging power (i.e. discharging) under the V2G function. The power capacity in a charging hub is determined by the capacity of sub-station, inverters, converters, wires, and other factors. A higher power capacity usually comes with a higher cost. In a shared charging hub, EBs and EVs can share common power facilities. When their charging schedules are coordinated to reduce the maximum combined charging power, the required power capacity in a charging hub can potentially be reduced, leading to significant cost savings.

4.3.4 Number of Chargers

$$N_k^b \geq n_{kt}^b, \quad \forall k \in K, \forall t \in T \tag{18}$$

$$N_k^v \geq n_{kt}^v, \quad \forall k \in K, \forall t \in T, \tag{19}$$

$$n_{kt}^b = \sum_{i \in I} \hat{x}_{ikt}, \quad \forall k \in K, \forall t \in T, \tag{20}$$

$$n_{kt}^v = \sum_{j \in J} \hat{y}_{jkt}, \quad \forall k \in K, \forall t \in T, \tag{21}$$

$$\hat{x}_{ikt} = \begin{cases} 1, & \text{if } \beta_{ikt} x_{it} \neq 0 \\ 0, & \text{otherwise,} \end{cases} \tag{22}$$

$$\hat{y}_{jkt} = \begin{cases} 1, & \text{if } \gamma_{jkt} y_{jt} \neq 0 \\ 0, & \text{otherwise,} \end{cases} \tag{23}$$

In addition to power capacity, the number of chargers should also match the charging demands. Constraints (18) and (19) require that the number of installed EB chargers N_k^b and EV chargers N_k^v should be no less than the number of in-use chargers at any time, where n_{kt}^b and n_{kt}^v are the number of EB and EV chargers in-use at time t, respectively. A binary variable $\hat{x}_{ikt}$ is introduced to indicate whether a bus i is connected to a charger in charging hub k at time t. As shown in constraint (22), $\hat{x}_{ikt} = 1$ if the following two conditions are true: a) Bus i is dwelling at charging hub k at time t, i.e. $\beta_{ikt} = 1$, b) Bus i has none-zero charging power, either being charged or discharged, i.e. $x_{it} \neq 0$. When $\hat{x}_{ikt} = 1$, bus i must be occupying one EB charger at charging hub k. Then the number of in-use EB chargers at time t is the sum of $\hat{x}_{ikt}$ over the set I of buses, as shown in constraint (20). Similar relationships between n_{kt}^v and $\hat{y}_{jkt}$ can be found in constraints (21) and (23) for EVs.

4.3.5 Investment Decision on Candidate Charging Hubs

$$\hat{N}_k = \begin{cases} 1, & \text{if } N_k^b + N_k^v > 0 \\ 0, & \text{otherwise} \end{cases} \tag{24}$$

When the number of EB chargers or EV chargers is greater than zero, a candidate charging hub is said to be deployed or built, indicated by a binary variable $\hat{N}_k$ as shown in constraint (24). In other words, if a charging hub k is not established, i.e. $\hat{N}_k = 0$, then both of N_k^b and N_k^v are zero. As a result, no EBs or EVs can get charged at charging hub k according to constraints (18)-(23). How the deployment of a charging hub constrains the charging of EBs and EVs is explained as follows. Taking EB for example, $N_k^b = 0$ indicates that $n_{kt}^b = 0, \forall t \in T$ according to (18), as n_{kt}^b is the sum of non-negative numbers. In this case, $\hat{x}_{ikt}$ must be 0 , $\forall i \in I, t \in T$, i.e. $\beta_{ikt} x_{it} = 0, \forall i \in I, t \in T$. This can be broken down into two scenarios. First, if $\beta_{ikt} = 1$, then x_{it} must be zero. Second, if $\beta_{ikt} = 0$, this means that the bus is not dwelling in the charging hub k, so x_{it} must be zero according to constraint (8). Hence, when $\hat{N}_k = 0$, no EBs can be charged in this unbuilt charging hub. The same effect can be explained in a similar way for EVs.

4.3.6 Budget

$$\sum_{k \in K} (c^b N_k^b + c^v N_k^v + c^f \hat{N}_k + c^p P_k^{cap}) + \sum_{i \in I} c^{eb} z_i + D \sum_{t \in T} \sum_{i \in I} c_t^e x_{it} \Delta t \leq B, \tag{25}$$

The public transit agencies will lease EBs and charging infrastructure from private vendors on an annual basis. The overall project is constrained by an annual budget B, and the total annual cost consists of two categories: 1) Property-leasing cost, which includes cost of leasing EB chargers $\left(c^b N_k^b\right)$ and EV chargers $(c^v N_k^v)$, cost of leasing charging hubs $\left(c^f \hat{N}_k\right)$ and paying for enough power capacity $(c^p P_k^{cap})$, and cost of leasing electric buses $\left(c^{eb} z_i\right)$. 2) Operational cost, or electricity cost $(c_t^e x_{it})$, where D is the number of days in a year and c_t^e is the electricity price at time t.

4.3.7 Electricity Cost of EVs

$$D \left(\sum_{t \in T_j^{v,hub}} c_t^e y_{jt} + \sum_{t \in T_j^{home}} c_t^{e,home} y_{jt} + \sum_{t \in T} c^{deg} |y_{jt}| \right) \Delta t \leq C_j^{EV,min}, \forall j \in J \tag{26}$$

While EV chargers are covered by public budget, the EV owners are still supposed to pay for their own electricity usage. On the other hand, we also want to ensure that EVs are incentivized to participate in reducing GHG emissions. For this purpose, we require that the charging scheduling results will not lead to a cost higher than the minimal cost of home charging. This requirement is applicable to each individual EV, as shown in constraint (26), where $c_t^{e,home}$ is the electricity price of home charging, which can be different (usually lower) than that in the charging hub. For private EVs, battery degradation needs to be considered as a cost. This is in contrast with EBs, whose batteries are leased and the degradation cost is reflected in the leasing price. In (26), c^{deg} is the battery degradation cost for charging/discharging 1kWh of electricity. $C_j^{EV,min}$ is the annual minimal electricity cost of EV j and it can be obtained by slightly modifying and solving (10)-(14) with home charging only and with the objective of minimizing electricity cost. The process of obtaining $C_j^{EV,min}$ is included in Appendix A.

4.4 Summary of the Model

As a summary of the model formulation in this section, the model is solved under objective function (1) and subject to constraints (2) - (26). Specifically, (22), (23) and (24) will be linearized using standard techniques (see Appendix B) such that the optimization problem is transformed to a mixed-integer linear program (MILP), which can be handled by commercial solvers.

5 Data Description

5.1 Study Area

Contra Costa, California is selected as the study area to illustrate the effectiveness of the proposed model. The public ground transportation in this area is served by one rail agency (Bay Area Rapid Transit or BART) and seven bus agencies. There are twelve BART stations within Contra Costa. Serving as an efficient travel mode between Contra Costa and downtown San Francisco, BART connects with several bus lines and has a large demand of private vehicles to park-and-ride in the vicinity of its stations. Therefore, BART stations are ideal locations for shared charging hubs. We identify the twelve BART stations in Contra Costa as candidate charging hubs as shown in Figure 2.

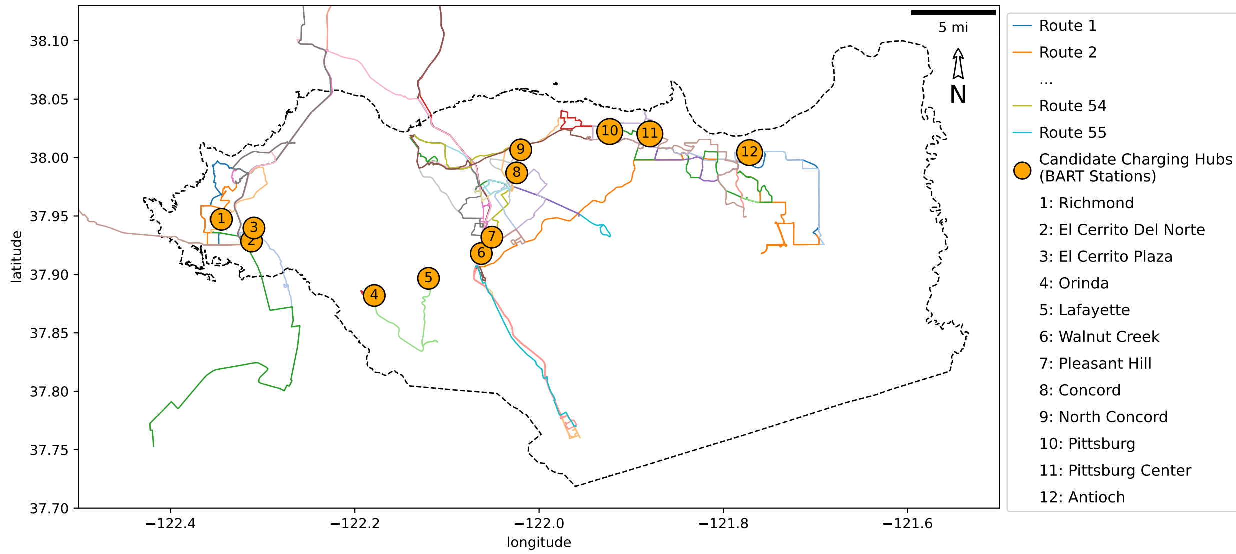

Figure 2: The selected bus routes and candidate charging hubs within the study area: Contra Costa, California.

5.2 Bus Sector

The data of bus sector is obtained from the General Transit Feed Specification (GTFS) of each transit agency [511 Open Data, 2021]. GTFS data consists of detailed information on bus routes, schedules, stops, and other necessary information. It is assumed that an EB can be charged in a charging hub if at least one of its terminal stations is within 0.5 miles of the charging hub. In such a scenario, the energy cost and time required to reach a charging hub from a nearby terminal is considered to be negligible. There are 55 identified bus routes, of which at least one terminal station is within 0.5 miles of a candidate charging hub, as shown in Figure 2.

While the schedule of a bus route can be extracted from the GTFS data, the information regarding individual buses that serve a route or their depot locations are unavailable to the public. A first-in-first-out (FIFO) model is adopted to address this problem [Ceder, 2016]. The FIFO model takes the schedule of a bus route as input and then outputs the required number of buses and the schedule of each bus on this route, by assuming: 1) no interlining of buses or deadhead trips (i.e. a bus only serves one specific route) and 2) a bus is at its depot during the longest break between services and in this case, the time returning to depot is neglected. Specifically, the FIFO model works as follows in determining the bus schedules for a two-terminal route: 1) A bus will be created at a terminal for the earliest scheduled trip; 2) Then this bus will make the first feasible connection with a departure after it has dwelt for more than 10 minutes at the other terminal of the route. Such connections will continue until this bus finishes the final applicable trip of the day; 3) Initiate a new bus for the earliest unassigned trip, and repeat steps 1) and 2) until all of the trips in the time table are assigned. After the three steps, we will obtain the number of buses serving this route and the detailed schedule of each bus. A similar process is also applicable to one-terminal routes, or round routes. The only change is in step 2) where the connection will happen in the same terminal. Through the FIFO model, a set I of 234 buses is obtained. It should be noted that the FIFO model could potentially exaggerate the number of buses. Reducing the number of buses through well-designed dispatching strategies is an ongoing research topic [Janovec and Kohâni, 2019, Kang et al., 2019, Li et al., 2019]. Nevertheless, the existing bus schedule is just an input into the modeling framework. The proposed framework can be equally applied once the actual detailed bus-level data becomes available.

For each bus i, we identify sets of departure time points $T_i^{departure}$, in-hub time points $T_i^{b,hub}$, in-terminal time points $T_i^{b,terminal}$, and in-depot time points T_i^{depot}. The in-depot time of a bus is determined to be the longest period between one arrival and the next departure. Also, the in-hub time points is a subset of in-terminal time points, i.e. $T_i^{b,hub} \subseteq T_i^{b,terminal}$, as an EB can only be charged in a hub when it is dwelling in a terminal according to the assumption made in Section 4.1.

Once the schedule of a bus is obtained, its daily GHG emission u_i can be estimated by assuming the current conventional bus fleet uses diesel as fuel. Based on the fuel efficiency of diesel buses η^d and the carbon intensity of diesel CI^d:

$$u_i = \frac{f_i \cdot d_i \cdot CI^d}{\eta^d}, \tag{27}$$

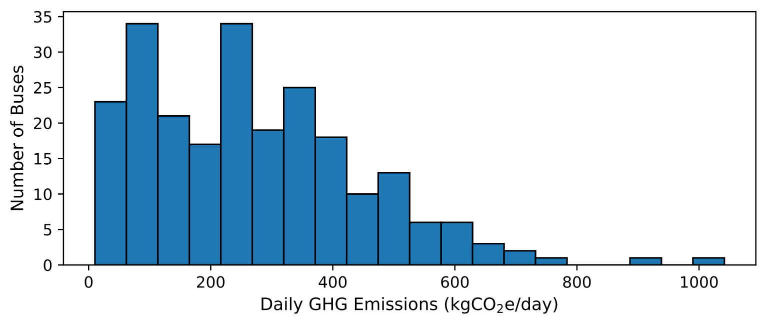

Figure 3: The distribution of daily GHG emissions of the bus fleet.

where f_i is the daily dispatch frequency. d_i is the one-way route distance. η^d is selected to be 3.26 miles/gallon [U.S. Department of Energy, 2021], and CI^d is 10.19 kgCO_2e/gallon [U.S. Environmental Protection Agency, 2021]. Figure 3 shows the histogram of GHG emissions of buses. Depending on the dispatch frequency and route distance, the daily GHG emissions of buses have wide variations, ranging from less than 50 kgCO_2e/day and up to more than 1,000 kgCO_2e/day.

When a conventional bus is converted to an EB, its battery capacity is assumed to be $e^{b,max} =$ 225kWh and $e^{b,min} =$ 22.5kWh. The maximum charging/discharging power is 150kW, i.e. $x^{max} =$ 150kW and $x^{min} = -$150kW. The energy efficiency of EBs η^b is 0.56 mile/kWh. The energy levels, charging power limits, and energy efficiency are selected based on information from the state-of-the-art bus vendor [Proterra, 2021]. The battery cycle efficiency κ is set at 0.95. The power consumption rate s_{it} is determined through the following approximation: an EB consumes zero energy when it is in a terminal or a depot. Otherwise, its power consumption rate s_{it} is a constant depending on the one-way distance, electricity fuel efficiency η^b, and the duration of running τ_i^t between two terminals, as shown in (28). Note that the duration of running between two terminals is time-dependent and it can vary during the day due to traffic conditions. This information is already reflected in the schedules derived from GTFS data.

$$s_{it}^b = \begin{cases} 0, & \text{if } t \in \{T_i^{b,terminal} \cup T_i^{depot}\} \\ d_i/(\eta^b \cdot \tau_i^t), & \text{otherwise,} \end{cases} \tag{28}$$

5.3 EV Sector

As the candidate charging hubs are located near the BART stations, the majority of users are expected to be EV drivers who park-and-ride. From the annual average hourly entry- and exit-pattern of the BART stations shown in Figure 4 [BART, 2021], it is found that leaving in the morning and returning in the evening is a clear pattern for BART riders in Contra Costa county. Assuming that park-and-ride EV drivers follow similar travel behavior, a stochastic Poisson arrival model for EVs can be established, with the hourly arrival rate in BART station k at hour h to be:

$$\lambda(k,h) = \text{Ridership}(k,h) \times \text{EV penetration rate} \times \text{park-and-ride rate}, \tag{29}$$

The EV penetration rate is set at 30% to reflect the growth of EV population in the near future. The park-and-ride rate is assumed to be 10%. Upon arrival, it is assumed that the parking time for EVs follows Gaussian distribution $\mathcal{N}(8, 2^2)$, i.e. the mean parking time is eight hours and the standard deviation is two hours. This is in-line with the exit pattern shown in Figure 4 (right). In total, a set J consisting of 1,527 individuals EVs is identified for the twelve BART stations.

The time horizon T is split into three parts for an EV j: at-home T_j^{home}, in-hub $T_j^{v,hub}$, or on-road for the rest of the time. An EV is on-road one hour before it arrives at the charging hub and one hour after it leaves the hub. An EV requires an energy supply that covers its daily consumption. As indicated by [Burns, 1979, Spillar, 1997, Holguı et al., 2012], the majority of park-and-ride users are located within 10 miles of the facility. Hence, the daily travel distance of an EV is a stochastic number generated by following the distribution of vehicle daily travel distance in the National Household Travel Survey [Federal Highway Administration, 2017], excluding the population that travel more than 10 miles in

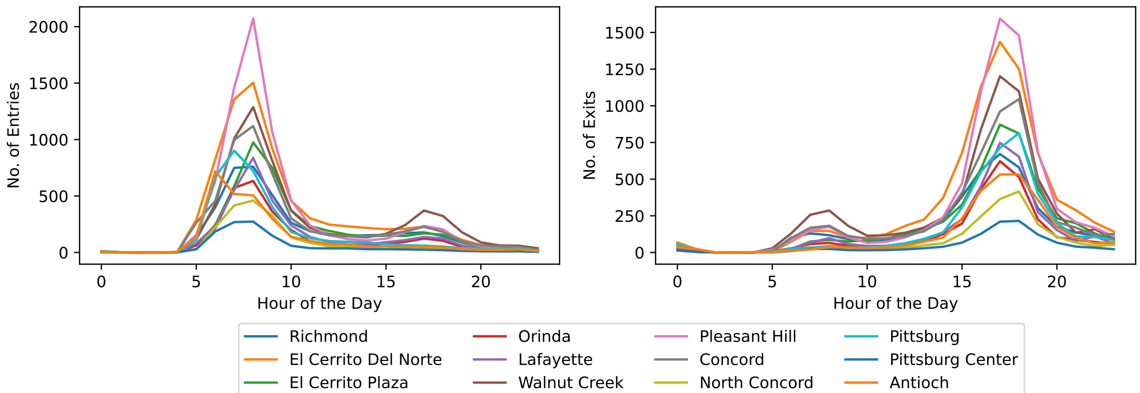

Figure 4: The annual average number of entries (left) and exits (right) of twelve BART stations in Contra Costa, California.

one-way trips. Similar to (28) for EBs, the power consumption rate of EVs s^v_{jt} is determined by the daily travel distance and the electricity fuel efficiency of EVs η^v (3.33 mile/kWh [Eco Cost Savings, 2021]).

EVs have options to be charged either at home with low-power AC chargers or at the charging hubs with DC-fast chargers, both having V2G functions. The maximum charging/discharging power is 50kW in a charging hub and 10kW at home, i.e. $y^{max} = 50\text{kW}$, $y^{min} = -50\text{kW}$, $y^{home,max} = 10\text{kW}$, and $y^{home,min} = -10\text{kW}$. Without the loss of generality, an EB's battery capacity is assumed to be $e^{v,max} = 100\text{kWh}$ and $e^{v,min} = 10\text{kWh}$. The battery cycle efficiency of charging EV batteries is the same as EBs.

5.4 Electricity Carbon Intensity

Electricity carbon intensity (ECI) measures the amount of GHG emissions by generating one kWh of electricity. In the previous literature, there are two types of ECIs adopted to study the GHG reduction of EVs, namely average and marginal ECI. The average ECI is derived by taking the weighted average emission factors of all electricity generation units at a certain time point [Dixon et al., 2020, Santarromana et al., 2020], while the marginal ECI is determined by the generation units that are responding to the near-term increase in electricity demand [Hoehne and Chester, 2016, Tu et al., 2020]. The average ECI is suitable for GHG emission auditing purposes, and the marginal ECI is believed to be more accurate in near-term charging optimization [Brinkel et al., 2020]. In this study, since the focus is long-term GHG reduction, the average ECI is chosen. If not specified, the ECI mentioned in the rest of this paper is the average ECI. In California, the calculation of ECI is relatively straightforward. California Independent System Operator (CAISO) [CAISO, 2021] provides the total real-time grid GHG emissions and power demand every 5 minutes. The ECI g_t at a time t can be obtained by dividing the total grid GHG emissions by the total power demand. The ECI of a typical day is shown in Figure 5. The lowest ECI is found around 9 AM-3 PM when the solar generations reach their peak. In the evenings and early mornings, the electricity is mainly generated by natural gases power plants, which led to higher ECI.

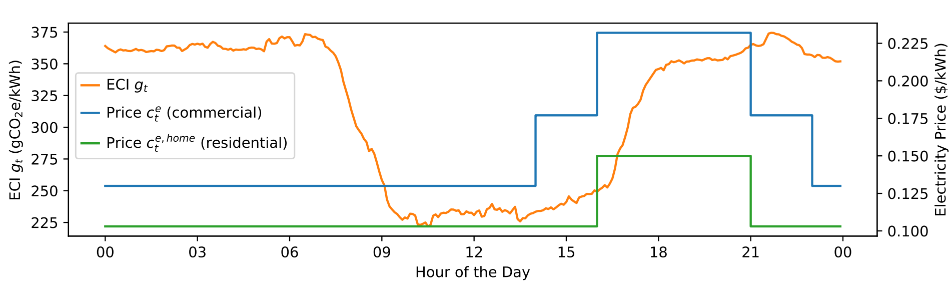

Figure 5: The electricity carbon intensity (ECI) and the electricity prices at different time of the day.

5.5 Cost

5.5.1 Property-leasing Cost

The leasing costs of charging infrastructure and EBs will be closely related to the lifespan of the properties. The annual leasing price c of a property is determined by that the net present value of leasing over the lifespan shall be no less than the initial investment:

$$c + \frac{c}{1+r} + \frac{c}{(1+r)^2} + ... + \frac{c}{(1+r)^{(n-1)}} \geq I_0, \tag{30}$$

where c is the annual leasing price, r is the interest rate, n is the lifespan of the property (in years), and I_0 is the initial investment of the property. Here we assume that the NPV is equal to the initial investment. By solving (30) with an equality sign, we will obtain $c \propto 1 - \frac{1}{(1+r)^n}$, from which we can infer that a shorter lifespan implies higher leasing cost.

The public transportation agencies will lease five different types of properties as stated in (25). The initial investment of an EB is taken from [Johnson et al., 2020]. An EB consists of a frame and a battery, which have different lifespans. While a frame can typically last 12-14 years [Noel and McCormack, 2014, Bi et al., 2017], a battery will need to be replaced every 6 to 8 years [Noel and McCormack, 2014, Franca et al., 2017]. A new lithium-ion battery will cost around \$140 per kWh [Edelstein, 2021] and as a result, an EB battery with a capacity of 225kWh will cost \$35,000. The initial investment of chargers are determined by multiple factors, including material and labor. [Nicholas, 2019, Nelder and Rogers, 2019] summarized the ranges of unit cost to install DC-Fast chargers. The lifespan of a charger is estimated to be 10 years. The initial investment of power equipment on a per-kW basis is derived from the cost of transformers and other necessary make-ready investments, including wires, conduits, meters, and etc. [Nelder and Rogers, 2019]. The lifespan of power equipment is estimated to be 20 years [Biçen et al., 2014]. The initial investment of a charging hub can vary from location to location, depending on the local real estate price, complexity of engineering, and other factors. For simplicity, here we assume that it is the same for the twelve candidate charging hubs and use 10 years as an estimated lifespan. Note that the model formulation allows us to use a different initial investment for each location if such information becomes available. Table 2 lists the initial investments, lifespans, and the resultant annual leasing costs for each property based on an annual interest rate of 10%.

Table 2: List of Initial Investments, Lifespans, and the Annual Leasing Costs

Property	**Initial Investment (\$)**	**Lifespan (years)**	**Leasing Cost (\$/year)**
EB charger (150kW)	100,000	10	14,795
EV charger (50kW)	30,000	10	4,439
Power equipment	200 (per kW)	20	21 (per kW)
Charging hub	1,000,000	10	147,950
EB, include: · Battery · Frame	900,000 35,000 865,000	- 6 12	122,715 7,306 115,409

5.5.2 Electricity Cost

Similar to ECI, electricity price varies across a day. Typically, utility companies will specify time-of-use schedules based on the load levels of the electricity market. The price will be higher during on-peak hours and lower during off-peak hours. The electricity prices are also different for commercial and residential users. While charging hubs will pay for a commercial rate, EVs performing home-charging will be billed under a residential rate. Typical commercial rates are higher than residential rates. We adopt the electricity prices from the service provider of Contra Costa [MCE, 2022], as shown in Figure 5.

5.5.3 Battery Degradation Cost

The degradation of a lithium-ion battery is impacted by multiple factors and it is a non-linear process. However, linearized degradation models could approximate the nonlinear model quite well [Foggo and Yu, 2017, Cardoso et al., 2018, Tang and Wang, 2022]. Here we assume that the degradation is proportional to the cycle numbers and the per kWh degradation cost c^{deg} is estimated through the following equation:

$$I_0^{battery} = 2 \cdot c^{deg} \cdot Cap \cdot DoD \cdot N^{cycle}, \quad (31)$$

where $I_0^{battery}$ is the initial investment of a new battery, Cap is the capacity of the battery, DoD is the cycling depth of discharge, and N^{cycle} is the end-of-life (EoL) cycle numbers of the battery. As suggested by [Ortega-Vazquez, 2014, Xu et al., 2016], N^{cycle} falls in the range of $2 \sim 3 \times 10^3$ at $DoD = 90\%$. Hence, we estimate $N^{cycle} = 2.5 \times 10^3$, and with the battery price $140 per kWh introduced in 5.5.1, we obtain $c^{deg} = \$0.031/kWh$ by solving (31).

6 Results and Discussion

This section presents the study results based on the optimization problem (1)-(26) and the input data introduced in Section 5. First of all, a comprehensive cost-benefit analysis is conducted to quantify the reductions of GHG emissions under different annual budget levels and how the budget is allocated to different sectors. Secondly, load profiles of charging hubs are presented and discussed, highlighting the benefit of the shared charging scheme. Thirdly, the impacts of considering time-varying ECI and V2G function in the operation are analyzed. Finally, a priority analysis is conducted to address the questions of resource allocations under budget limitations, providing necessary information to local decision-makers.

The optimization problem is solved using Gurobi solver on AWS cloud server with AMD CPUs. To balance the operational time accuracy requirement and the solver time, the control time intervals are set to be 5 minutes for the bus sector and 60 minutes for the EV sector. The study time horizon is one day.

6.1 Cost-Benefit Analysis

A cost-benefit analysis is conducted in this subsection to understand the potential of decarbonization under different annual budget levels. The optimization problem (1)-(26) is solved under a range of annual budget scenarios from $0 to $44 million. The level of decarbonization is measured by R, the reduction of GHG emissions. The value of R under a certain budget B' is calculated by $R(B = B') = U(B = B') - U(B = 0)$, i.e. the difference of GHG emissions between budget B' and $0. The latter case serves as a baseline for performance comparison. The overall results are presented in Figure 6. First of all, the total reduction of GHG emissions is increasing with the budget, as shown in Figure 6(a). The marginal benefits of having a higher budget gradually reduce as the total GHG reduction curve becomes flat with high budgets. Under the budget level of $44 million, the total GHG reduction is 62.6 metric tonnes CO_2e per day (mTCO_2e/day), in which the bus sector yields a reduction of 54.2 mTCO_2e/day or 86.6%, while the EV sector contributes to a reduction of 8.4 mTCO_2e/day or 13.4%. The results of other key parameters under different annual budget levels are presented in Figure 6(b)-(g). Figure 6(b) shows the number of deployed charging hubs. Figure 6(c) shows the number of leased EBs and the number of EVs that get charged in a charging hub. Figure 6(d) shows the number of EB and EV chargers. Figure 6(e) shows the total power capacity required for all charging hubs and the power demands for EB and EV sectors. Figure 6(f) and (g) presents the allocation of budgets in the form of absolute values and percentages, respectively. Based on the observation in Figure 6, system planning can be split into five phases:

- Phase 1: Budget $0-$2 million. In this phase, budget is mainly allocated to the EV sector. Specifically, when B = 2 million, 5 charging hubs are deployed as shown in Figure 6(b) and a significant amount of EVs are being charged in the charging hubs as shown in Figure 6(c), while the number of EBs and EB chargers are both limited, as shown in Figure 6(c) and (d). In this phase, the EV sector contributes more GHG reduction than the bus sector.
- Phase 2: Budget $2-$8 million. The development of the bus sector accelerates starting from B = 2 million. The amount of budget allocated to EBs outpaces the amount spent in EV chargers, as shown in Figure 6(g). The contribution to GHG reduction from the bus sector exceeds that from the EV sector.
- Phase 3: Budget $8-$34 million. In this phase, the bus sector continues to grow, while the EV sector is saturated. The number of EBs and EB chargers is increasing steadily with the budget, leading to significant GHG reductions in the bus sector. On the other hand, the GHG reduction from the EV sector has very limited improvement when the budget increases. The number of EVs that choose to charge in charging hubs reaches a high level in the early stage of this phase and grows slowly in later stages, as shown in Figure 6(c). Although the number of EV chargers continues to grow, it only eases the scheduling congestion of EV charging, with limited contribution to the GHG reduction. The majority of the budget is allocated to electrifying buses as shown in Figure 6(g).

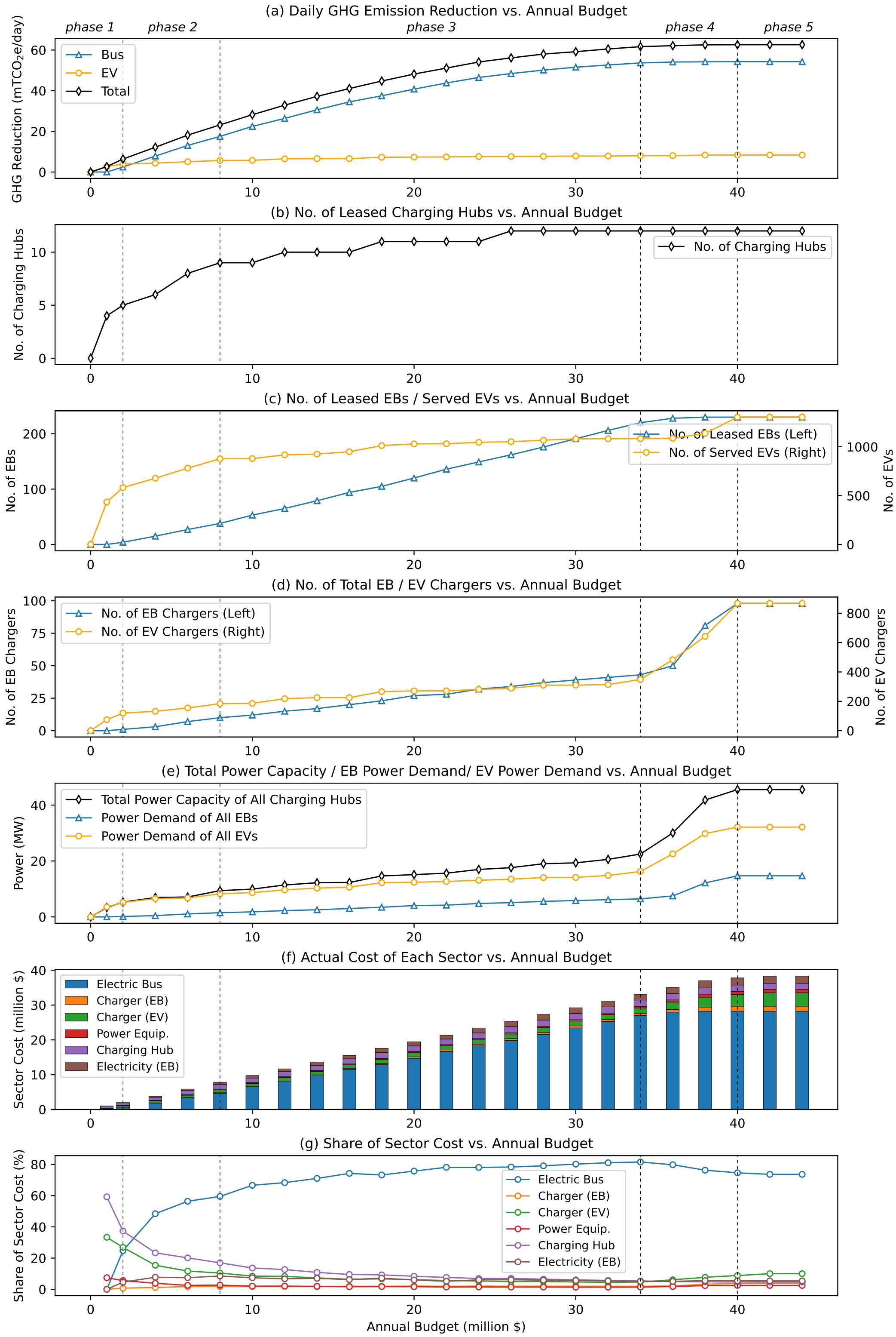

Figure 6: Overview of the planning results under different budget levels.

- Phase 4: Budget $34-$40 million. In this phase, the number of EB/EV chargers and the associated power capacity are soaring to accommodate a few EBs and EVs, as shown in Figure 6(d) and (e). While the budget increased significantly compared with phase 3, the GHG reduction has very limited improvement. This marks a significant drop in the marginal benefit of investment.

- Phase 5: Budget $40 million and above. When the budget reaches $40 million, both the bus sector and the EV sector are saturated. No more reduction of GHG emissions is observed as budget increases. All eligible conventional buses are converted to EBs. The constant number of chargers and power capacity indicates that the charging demand is fully satisfied. There are a few conventional buses that are not electrified, because of extremely long route distance or high frequency of dispatches.

Based on the above cost-benefit analysis, it is suggested that the investment should focus on phases 1 and 2, in which the marginal benefit is substantial. If more funding is provided, reaching a certain stage of phase 3 is also a good choice. However, investing heavily in phase 4 or 5 is not recommended as the marginal benefit is low.

6.2 The Advantages of Shared Charging Hubs

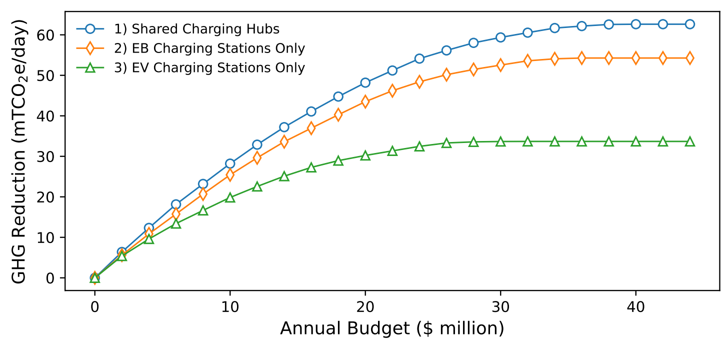

Figure 7: Reduction of GHG emissions under three different planning scenarios: 1) Shared charging hubs for both EBs and EVs, 2) EB charging stations only, and 3) EV charging stations only.

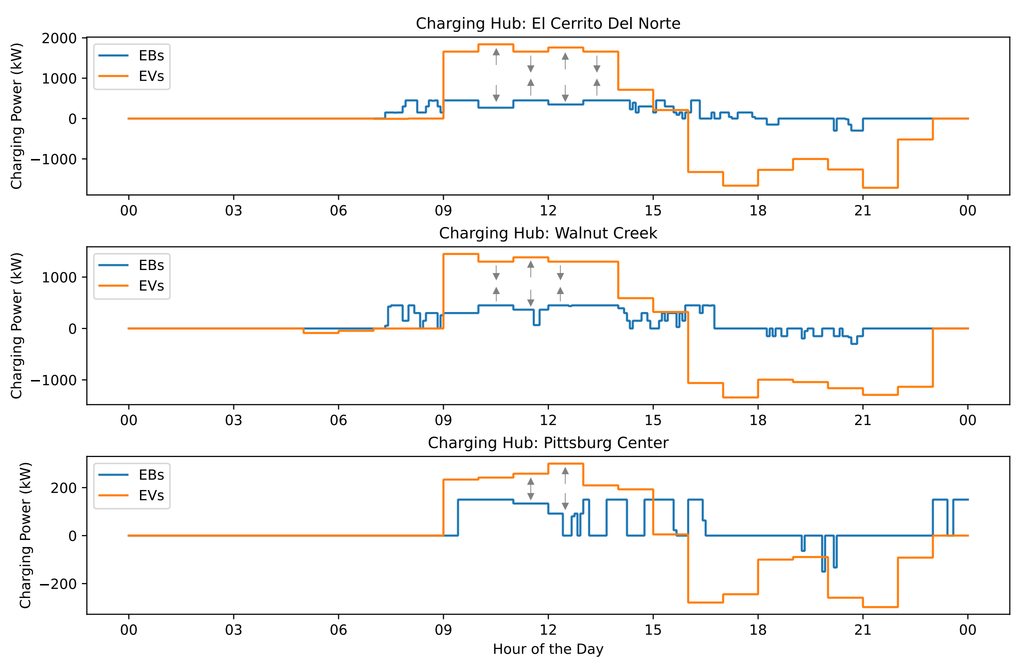

Figure 8: Load profiles of three charging hubs. Gray arrows indicate coordinated charging between EBs and EVs to limit the increase of total peak power demand.

In the proposed model, the planning of the bus and EV sectors are carried out in a collaborative manner through the scheme of shared charging hubs. Here we illustrate how such a scheme improves the overall reduction of GHG emissions. To make this point, a comparison between the shared and the isolated charging schemes is conducted. The proposed model is solved under three different schemes: 1) Shared charging hubs, 2) EB charging stations only, and 3) EV charging stations only. For scheme 2, the number of EV chargers is set to be zero, i.e. $N_k^v = 0, \forall k \in K$. Similarly, for scheme 3, the number of EB chargers is set to be zero, i.e. $N_k^b = 0, \forall k \in K$. The reductions of GHG emissions of these three schemes under different budget levels are shown in Figure 7. First of all, it is noticed that under low budget levels, the GHG reductions for schemes 1, 2 and 3 are very close, indicating that developing either EB or EV charging stations is equally as good as developing shared charging hubs. However, in scheme 2 when the budget increases, the marginal benefit of EB charging stations decreases faster than scheme 1. The performance of Scheme 3 is even less ideal in the high budget region. Actually, in the high budget region of scheme 3, most of the GHG reduction is contributed by electrifying buses that can be operated without terminal charging (with depot charging only). This can be inferred from Figure 6(a) where the GHG reduction from the EV sector is saturated at low budget levels. On the other hand, though the marginal benefits of scheme 2 is similar to scheme 3 at low budget levels, the growth of GHG reduction in scheme 2 is faster in high budget levels compared to scheme 3, because the establishment of EB charging stations makes it possible for more buses to be converted to EBs. Overall, the shared charging hubs of scheme 1 show the best performance under various budget levels among the three schemes. The reason behind the superior performance of scheme 1 is that with shared charging hubs, the model can implicitly determine the optimal allocation of resources between the bus and EV sectors. This contrasts with the isolated charging stations, where the resources are entirely poured into a single transportation mode without the flexibility to achieve collaborative development across different modes.

Reducing peak power through coordinated charging is another potential benefit of the shared charging hubs. To analyze this effect, the charging powers of EB and EV sectors at different times of the day are presented in Figure 8 for three deployed charging hubs. The results are obtained under a budget of \$12 million. Based on the observation of Figure 8, the peak charging demands of EBs and EVs all occur around 9 AM-3 PM when both the ECI and the electricity cost are low due to excess power from solar plants, while discharging usually happens at night to offset GHG emissions when both the ECI and the electricity cost are high. An interesting phenomenon is that neither charging or discharging is preferred in the early morning, as the signals of ECI and electricity price contradict each other. During the period of peak charging demand, clear patterns of coordinated charging can be found in all of the three charging hubs, as indicated by the gray arrows in Figure 8. Taking charging hub El Cerrito Del Norte as an example, there are two outstanding peak stages of EVs' charging power between 9 AM-3 PM, correspondingly, the charging power of EBs experience two valleys at the same time as the peaks of EVs, such that the peak power of the charging hub is not exceeded. Similar phenomena can be observed in the other two charging hubs. Keeping peak power consumption at a low level has multiple benefits. On one hand, the initial capital required for power equipment is reduced immediately. This effect has been considered in the proposed model. On the other hand, the charging hubs will receive lower electricity bills due to reduced peak demand charges, which implies profound benefit in the long run.

6.3 The Impacts of ECI and V2G

The time-varying ECI and V2G technology are included in the proposed planning model. In this subsection, we quantify their contributions to the decarbonization effort. To do this, the proposed planning problem is solved under three different settings: 1) with awareness of time-varying ECI and V2G is enabled (w/ ECI, w/ V2G), 2) with awareness of time-varying ECI, but V2G is disabled (w/ ECI, w/o V2G), 3) without awareness of time-varying ECI and V2G is disabled (w/o ECI, w/o V2G). For case 2, the proposed planning problem is solved by setting $x^{min} = 0$, $y^{min} = 0$, and $y^{home,min} = 0$ in (7), (12), and (13), respectively, i.e. not allowing discharging from EBs or EVs. For case 3, besides the modifications made in case 2, the daily average ECI $\bar{g}$ is adopted to replace g_t in (2) and (3), where $\bar{g} = \frac{1}{|T|}\sum_{t\in T} g_t$ is a constant throughout the study time horizon T ($|T|$ measures the number of time steps in T), such that the modified model is unaware of the time-varying ECI and charging at different time of the day makes no difference to its objective function (1). After obtaining the optimization results for case 3, its actual GHG emissions are calculated based on the time-varying ECI. In most of the existing charging infrastructure, there is no ECI-oriented scheduling or V2G function. This situation is represented by case 3.

Figure 9(a) shows the GHG emission reductions of the above three cases under different budget levels. Using case 3 as the baseline, a considerable improvement of GHG reduction is observed when the time-varying ECI is considered in case 2. Further enabling the V2G in case 1 results in an even more significant improvement. Taking the budget of \$30 million as an example, the GHG reductions are 59.4, 50.6, and 47.8 $mTCO_2e$/day, for cases 1, 2, and 3, respectively. The awareness of time-varying ECI increases the GHG reduction by 5.8% from case 3 to case 2. The better performance in case 2 comes from the optimized charging schedule that avoids charging in high ECI periods. Enabling V2G further increases the GHG reduction by 17.3% from case 2 to case 1, and 24.1% from case 3 to case 1. The reason behind such a substantial improvement is that the V2G function allows discharging EBs/EVs to serve the demand of the grid, such that less electricity is requested from power generation units. This is especially meaningful when the ECI is high. It

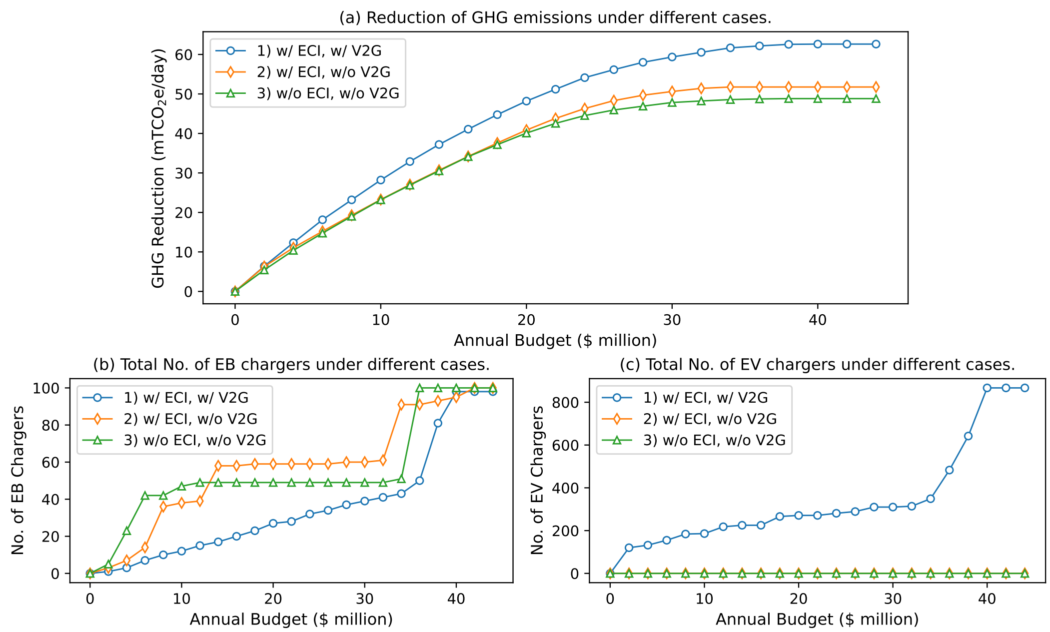

Figure 9: The impacts of time-varying ECI and V2G to the (a) GHG reductions, (b) required number of EB chargers, and (c) required number of EV chargers.

should be noted that the V2G function is only beneficial when there is awareness of time-varying ECI, which serves as the triggering signal of charging or discharging.

Comparing the planning results under different settings provides additional insights. By checking the total number of EB chargers shown in Figure 9 (b), it is found that more EB chargers are installed in cases 2 and 3 compared with case 1. The reason behind is that when the V2G function is disabled, the EV owners will find it uneconomical to use the charging hubs where the electricity price is high, but selling electricity through V2G is not feasible. In this case, most of the budget will be devoted to the bus sector. This can be inferred from Figure 9 (c) where EV chargers are not getting attention in case 2/3. The large difference in the number of EV chargers between case 1 and case 2/3 also points to the additional benefit provided by EVs in the system as energy storage units. When there is no V2G function as in case 2/3, the relative importance of the EV sector is reduced significantly.

6.4 Priority Analysis

The available budget is usually limited for the initial deployment of charging infrastructure. Under such circumstances, identifying the priorities of investment and development in different sub-sectors can greatly assist the decision making of policymakers. For this purpose, the planning results under four relatively low budget levels ($0.5, 1, 2, and 4 million) are analyzed in this subsection. The deployed charging hubs, the number of EB/EV chargers in these charging hubs, and the routes in which at least one bus is electrified are presented in Figure 10. At low budget levels, e.g $0.5 and 1 million, all of the budget is allocated to lease charging hubs and EV chargers, as indicated in Figure 10 (a) and (b). The first EB and EB charger is introduced when the budget is $2 million as shown in Figure 10 (c). Further increasing the budget to $4 million results in more EBs, but the increase of EB chargers is moderate. For example, when there are 15 EBs, only three EB chargers are needed as shown in Figure 10 (d), benefiting from the optimized charging schedules. Table 3 lists the planned number of EB/EV chargers in each candidate charging hub. A worth-mentioning phenomenon is that when budget increases, the number of EV chargers in a deployed charging hub remains largely unchanged. One of the possible explanations is that when the budget increases, new charging hubs are deployed such that the marginal benefit of adding EV chargers in the new charging hubs is greater than that of the existing charging hubs.

In terms of deciding which buses have higher priorities to be electrified, a straightforward idea is to select those that have higher daily GHG emissions. However, there are other factors that can affect this rule. Table 4 lists the top buses ranked by daily GHG emissions. Generally speaking, the order of a bus being electrified when the budget increases follows the order of its daily GHG emissions, but buses 65, 41, and 163 are exceptions as shown in Table 4. By checking each bus in detail, two reasons are found that prevent the electrification of a bus with high daily GHG emissions. One reason is the operation limits of buses, represented by buses 65 and 41. Bus 65 is dispatched nine times a day

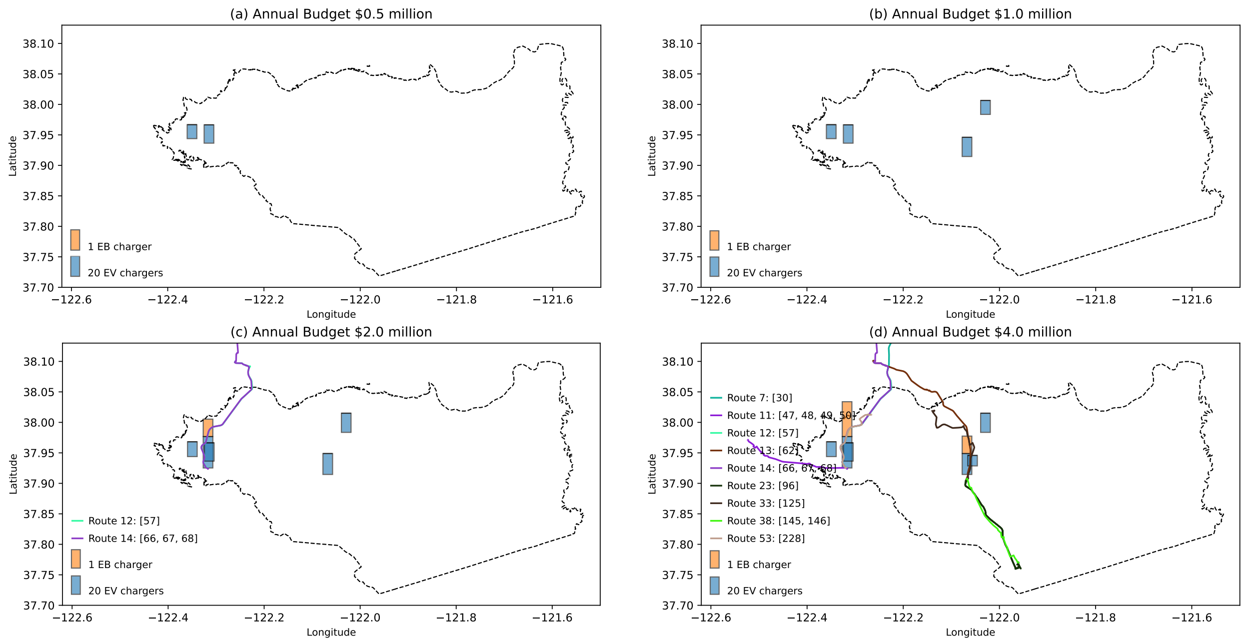

Figure 10: Planning results under four low budget levels: deployed charging hubs, number of EB/EV chargers, and bus routes with buses being electrified. Each vertical bar represents a deployed charging hub and the height of the bar indicates the number of EB/EV chargers leased in this charging hub. The individual buses being electrified are listed behind its route ID and the format is "Route ID: [Bus ID1, Bus ID2, ...]".

Table 3: List of deployed charging hubs and number of EB/EV chargers.

Candidate Charging Hub ID	Candidate Charging Hub Name	No. of EB/EV Chargers			
		Annual Budget ($ Million)			
		0.5	1	2	4
1	Richmond	0/16	0/16	0/17	0/17
2	El Cerrito Del Norte	-	-	1/36	2/36
3	El Cerrito Plaza	0/21	0/21	0/21	0/21
4	Orinda	-	-	-	-
5	Lafayette	-	-	-	-
6	Walnut Creek	-	0/22	0/24	1/24
7	Pleasant Hill	-	-	-	0/12
8	Concord	-	0/16	0/22	0/22
9	North Concord	-	-	-	-
10	Pittsburg	-	-	-	-
11	Pittsburg Center	-	-	-	-
12	Antioch	-	-	-	-

resulting in a total of more than five hundred miles of travel distance. Bus 41 has a one-way travel distance of more than seventy miles and its dwelling time in BART Walnut Creek is only 14 minutes. As a result, the currently available battery capacity and charging power fail to satisfy the electricity demand of buses 65 and 41. Another reason is that the corresponding charging hub has not been deployed, represented by bus 163. The applicable charging hub for bus 163 is BART Pittsburg Center, which has not been deployed due to budget limit. This means that electrifying bus 163 requires leasing a charging hub at BART Pittsburg Center at the same time, leading to a higher bundled cost compared to electrifying bus 96 that uses an existing charging hub.

Table 4: Rank of buses based on daily GHG emission and analysis of planning results.

Bus ID	Route ID	Agency, Route Name Terminal Stations	Emission ($kgCO_2e$/day)	Budget Level When Electrified ($ Million)	Reason Not Electrified
65	14	SolTran, R BART El Cerrito Del Norte - Suisun City	1042		High frequency dispatches
66	14	SolTran, R BART El Cerrito Del Norte - Suisun City	926	2.0	
57	12	SolTran, R BART El Cerrito Del Norte - Vallejo	736	2.0	
41	9	Fairfield and Suisun, BLUE BART Walnut Creek - Sacramento	708		Long route distance and short dwelling time at terminal
68	14	SolTran, R BART El Cerrito Del Norte - Suisun City	694	2.0	
62	13	SolTran, Y BART Walnut Creek - Vallejo	644	4.0	
145	38	The County Connection, 21 BART Walnut Creek - San Ramon	635	4.0	
163	41	TriDelta, 391 BART Pittsburg Center - Brentwood Park & Ride	631		Charging hub Pittsburg Center BART has not been deployed.
96	23	The County Connection, 96X BART Walnut Creek - Bishop Ranch	615	4.0	

7 Conclusion

This study focuses on the optimal deployment and operation of the shared charging hubs and the electrification of public transits to decarbonize the transportation sector within a regional area. With the objective to minimize the GHG emissions under given budgets, the optimization problem jointly determines which bus in the fleet shall be electrified, the locations of the charging hubs, and the necessary number of chargers and level of power capacities in these charging hubs. The optimization problem also determines coordinated charging schedules, which are developed with awareness of the time-varying ECI, electricity prices, and battery degradation, and largely benefited from the utilization of V2G technology.

Based on the results of the case study, there are several interesting aspects worth highlighting: (1) The development of charging infrastructure and electric bus fleets is roughly split into five different phases, in which the preferences and focuses of development are different. (2) The shared charging hubs enables coordinated charging between EBs and EVs, reducing the peak power demands in charging hubs and leading to savings in both initial capital investment of power equipment and long-term peak demand charges. (3) A lack of awareness of time-varying ECI or the V2G function will decrease the effectiveness of decarbonization and also result in drastically different allocations of resources. (4) Under relatively low budget levels, once a charging hub is initially deployed, increasing the budget does not increase the number of EV chargers in this charging hub because higher marginal benefits of adding EV chargers are generally found in newly deployed charging hubs. (5) The priority of electrifying conventional buses generally follows the ranking of the buses' daily GHG emissions. However, if constrained by operation limits or if there is a high bundled cost, a bus may not be electrified even if it has high daily GHG emissions.

It is worthwhile to mention the control of charging schedules. While the EB charging schedules can be predetermined given their fixed operation schedules, the day-to-day random arrivals and departures of EVs require online scheduling algorithms to achieve coordinated charging in real-world applications. The use of off-line optimization in this study is intended to provide an initial evaluation of the decarbonization potential. The development of online control algorithms with the proposed model is a promising future research direction.

Acknowledgments

This study was made possible through funding received by the University of California Institute of Transportation Studies from the State of California through the Public Transportation Account and the Road Repair and Accountability Act of 2017 (Senate Bill 1). The contents of this report reflect the views of the author(s), who is/are responsible for the facts and the accuracy of the information presented. This document is disseminated under the sponsorship of the State

of California in the interest of information exchange and does not necessarily reflect the official views or policies of the State of California.

References

[511 Open Data, 2021] 511 Open Data (2021). 511 SF Bay's Open Data Portal. [online] Available at:. https://511.org/open-data/transit. Accessed June 2021.

[BART, 2021] BART (2021). Ridership Reports, Bay Area Rapid Transit. [online] Available at:. https://www.bart.gov/about/reports/ridership. Accessed June 2021.

[Bi et al., 2017] Bi, Z., De Kleine, R., and Keoleian, G. A. (2017). Integrated life cycle assessment and life cycle cost model for comparing plug-in versus wireless charging for an electric bus system. *Journal of Industrial Ecology*, 21(2):344–355.

[Biçen et al., 2014] Biçen, Y., Aras, F., and Kirkici, H. (2014). Lifetime estimation and monitoring of power transformer considering annual load factors. *IEEE Transactions on Dielectrics and Electrical Insulation*, 21(3):1360–1367.

[Brinkel et al., 2020] Brinkel, N., Schram, W., AlSkaif, T., Lampropoulos, I., and Van Sark, W. (2020). Should we reinforce the grid? Cost and emission optimization of electric vehicle charging under different transformer limits. *Applied Energy*, 276:115285.

[Burns, 1979] Burns, E. (1979). Priority rating of potential park-and-ride sites. *ITE journal*, 49(2).

[CAAM, 2022] CAAM (2022). Automotive Statistics of China Association of Automobile Manufacturers. [online] Available at:. http://en.caam.org.cn/Index/lists/catid/27.html. Accessed Jan 2022.

[CAISO, 2021] CAISO (2021). California ISO: Today's Outlook - Emissions. [online] Available at:. http://www.caiso.com/todaysoutlook/pages/emissions.html. Accessed 21 October 2021.

[CALSTART, 2021] CALSTART (2021). Zeroing in on ZEBs. [online] Available at:. https://calstart.org/wp-content/uploads/2022/01/2021-ZIO-ZEB-Final-Report_1.3.21.pdf. Accessed Jan 2022.

[CARB, 2019] CARB (2019). Innovative Clean Transit (ICT) regulation fact sheet, the California Air Resources Board (CARB). [online] Available at:. https://ww2.arb.ca.gov/resources/fact-sheets/innovative-clean-transit-ict-regulation-fact-sheet. Accessed Jan 2022.

[Cardoso et al., 2018] Cardoso, G., Brouhard, T., DeForest, N., Wang, D., Heleno, M., and Kotzur, L. (2018). Battery aging in multi-energy microgrid design using mixed integer linear programming. *Applied energy*, 231:1059–1069.

[Ceder, 2016] Ceder, A. (2016). *Public transit planning and operation: Modeling, practice and behavior*. CRC press.

[Chen et al., 2018] Chen, Z., Yin, Y., and Song, Z. (2018). A cost-competitiveness analysis of charging infrastructure for electric bus operations. *Transportation Research Part C: Emerging Technologies*, 93:351–366.

[Dixon et al., 2020] Dixon, J., Bukhsh, W., Edmunds, C., and Bell, K. (2020). Scheduling electric vehicle charging to minimise carbon emissions and wind curtailment. *Renewable Energy*, 161:1072–1091.

[Doll, 2022] Doll, S. (2022). Introducing ZiGGY: An autonomous robot that saves you a parking spot then charges your EV. [online] Available at:. https://electrek.co/2022/06/14/ziggy-autonomous-robot-charges-ev/. Accessed Jun 2022.

[Eco Cost Savings, 2021] Eco Cost Savings (2021). Electric Car kWh Per Mile List. [online] Available at:. https://ecocostsavings.com/electric-car-kwh-per-mile-list/. Accessed June 2021.

[Edelstein, 2021] Edelstein, S. (2021). EV battery costs hit another low in 2021, but they might rise in 2022. [online] Available at:. https://www.greencarreports.com/news/1134307_report-ev-battery-costs-might-rise-in-2022. Accessed May 2022.

[Electrification Coalition, 2010] Electrification Coalition (2010). Fleet Electrification Roadmap. Revolutionizing Transportation and Achieving Energy Security. [online] Available at:. https://www.electrificationcoalition.org/fleet-electrification-roadmap-revolutionizing-transportation-and-achieving-energy-security/. Accessed Jun 2022.

[Federal Highway Administration, 2017] Federal Highway Administration (2017). National Household Travel Survey (NHTS) 2017. [online] Available at:. https://nhts.ornl.gov/. Accessed June 2021.

[Foggo and Yu, 2017] Foggo, B. and Yu, N. (2017). Improved battery storage valuation through degradation reduction. *IEEE Transactions on Smart Grid*, 9(6):5721–5732.

[Frade et al., 2011] Frade, I., Ribeiro, A., Gonçalves, G., and Antunes, A. P. (2011). Optimal location of charging stations for electric vehicles in a neighborhood in Lisbon, Portugal. *Transportation Research Record*, 2252(1):91–98.

[Franca et al., 2017] Franca, A., Fernandez, J. A., Crawford, C., and Djilali, N. (2017). Assessing the impact of an electric bus duty cycle on battery pack life span. In *2017 IEEE Transportation Electrification Conference and Expo (ITEC)*, pages 679–683. IEEE.

[Gerritsma et al., 2019] Gerritsma, M. K., AlSkaif, T. A., Fidder, H. A., and van Sark, W. G. (2019). Flexibility of electric vehicle demand: Analysis of measured charging data and simulation for the future. *World Electric Vehicle Journal*, 10(1):14.

[Ghamami et al., 2020] Ghamami, M., Kavianipour, M., Zockaie, A., Hohnstadt, L. R., and Ouyang, Y. (2020). Refueling infrastructure planning in intercity networks considering route choice and travel time delay for mixed fleet of electric and conventional vehicles. *Transportation Research Part C: Emerging Technologies*, 120:102802.

[Gohlke and Zhou, 2021] Gohlke, D. and Zhou, Y. (2021). Assessment of light-duty plug-in electric vehicles in the united states, 2010–2020. Technical report, Argonne National Lab.(ANL), Argonne, IL (United States).

[Hoehne and Chester, 2016] Hoehne, C. G. and Chester, M. V. (2016). Optimizing plug-in electric vehicle and vehicle-to-grid charge scheduling to minimize carbon emissions. *Energy*, 115:646–657.

[Holguı et al., 2012] Holguı, J., Yushimito, W. F., Aros-Vera, F., Reilly, J. J., et al. (2012). User rationality and optimal park-and-ride location under potential demand maximization. *Transportation Research Part B: Methodological*, 46(8):949–970.

[Janovec and Kohání, 2019] Janovec, M. and Kohání, M. (2019). Exact approach to the electric bus fleet scheduling. *Transportation Research Procedia*, 40:1380–1387.

[Jattin, 2019] Jattin, M. G. (2019). Financial Mechanisms for Electric Bus Adoption). [online] Available at:. https://www.changing-transport.org/wp-content/uploads/2019_Busfleet_Modernisation_Financial_Mechanisms.pdf. Accessed Jun 2022.

[Johnson et al., 2020] Johnson, C., Nobler, E., Eudy, L., and Jeffers, M. (2020). Financial analysis of battery electric transit buses. Technical report, National Renewable Energy Lab.(NREL), Golden, CO (United States).

[Jung et al., 2014] Jung, J., Chow, J. Y., Jayakrishnan, R., and Park, J. Y. (2014). Stochastic dynamic itinerary interception refueling location problem with queue delay for electric taxi charging stations. *Transportation Research Part C: Emerging Technologies*, 40:123–142.

[Kane, 2022] Kane, M. (2022). Norway sets plug-in car sales record for the end of the year 2021. [online] Available at:. https://insideevs.com/news/558447/norway-plugin-car-sales-december2021/. Accessed Jan 2022.

[Kang et al., 2019] Kang, L., Chen, S., and Meng, Q. (2019). Bus and driver scheduling with mealtime windows for a single public bus route. *Transportation Research Part C: Emerging Technologies*, 101:145–160.

[Kavianipour et al., 2021] Kavianipour, M., Fakhrmoosavi, F., Singh, H., Ghamami, M., Zockaie, A., Ouyang, Y., and Jackson, R. (2021). Electric vehicle fast charging infrastructure planning in urban networks considering daily travel and charging behavior. *Transportation Research Part D: Transport and Environment*, 93:102769.

[Kontou et al., 2019] Kontou, E., Liu, C., Xie, F., Wu, X., and Lin, Z. (2019). Understanding the linkage between electric vehicle charging network coverage and charging opportunity using GPS travel data. *Transportation Research Part C: Emerging Technologies*, 98:1–13.

[Kunith et al., 2017] Kunith, A., Mendelevitch, R., and Goehlich, D. (2017). Electrification of a city bus network—an optimization model for cost-effective placing of charging infrastructure and battery sizing of fast-charging electric bus systems. *International Journal of Sustainable Transportation*, 11(10):707–720.

[Lesh, 2013] Lesh, M. C. (2013). Innovative concepts in first-last mile connections to public transportation. In *Urban public transportation systems 2013*, pages 63–74.

[Li et al., 2019] Li, L., Lo, H. K., and Xiao, F. (2019). Mixed bus fleet scheduling under range and refueling constraints. *Transportation Research Part C: Emerging Technologies*, 104:443–462.

[Li et al., 2018] Li, X., Castellanos, S., and Maassen, A. (2018). Emerging trends and innovations for electric bus adoption—a comparative case study of contracting and financing of 22 cities in the americas, asia-pacific, and europe. *Research in Transportation Economics*, 69:470–481.

[Lin et al., 2019] Lin, Y., Zhang, K., Shen, Z.-J. M., Ye, B., and Miao, L. (2019). Multistage large-scale charging station planning for electric buses considering transportation network and power grid. *Transportation Research Part C: Emerging Technologies*, 107:423–443.

[Liu et al., 2017] Liu, Z., Song, Z., and He, Y. (2017). Optimal deployment of dynamic wireless charging facilities for an electric bus system. *Transportation Research Record*, 2647(1):100–108.

[López et al., 2015] López, M. A., De La Torre, S., Martín, S., and Aguado, J. A. (2015). Demand-side management in smart grid operation considering electric vehicles load shifting and vehicle-to-grid support. *International Journal of Electrical Power & Energy Systems*, 64:689–698.

[Lunden, 2018] Lunden, I. (2018). BYD and Generate Capital launch $200M electric bus leasing JV in the US). [online] Available at:. https://techcrunch.com/2018/07/11/byd-and-generate-capital-launch-200m-electric-bus-leasing-jv-in-the-us/. Accessed Jun 2022.

[Lutsey and Sperling, 2009] Lutsey, N. and Sperling, D. (2009). Greenhouse gas mitigation supply curve for the United States for transport versus other sectors. *Transportation Research Part D: Transport and Environment*, 14(3):222–229.

[MCE, 2022] MCE (2022). MCE Clean Energy. [online] Available at:. https://www.mcecleanenergy.org/. Accessed Jun 2022.

[Moon et al., 2020] Moon, J., Kim, Y. J., Cheong, T., and Song, S. H. (2020). Locating battery swapping stations for a smart e-bus system. *Sustainability*, 12(3):1142.

[Nelder and Rogers, 2019] Nelder, C. and Rogers, E. (2019). Reducing EV charging infrastructure costs. *Rocky Mountain Institute*.

[Nicholas, 2019] Nicholas, M. (2019). Estimating electric vehicle charging infrastructure costs across major US metropolitan areas. *URL: https://theicct. org/sites/default/files/publications/ICCT_EV_Charging_Cost_20190813. pdf*.

[Noel and McCormack, 2014] Noel, L. and McCormack, R. (2014). A cost benefit analysis of a V2G-capable electric school bus compared to a traditional diesel school bus. *Applied Energy*, 126:246–255.

[Obergassel et al., 2016] Obergassel, W., Arens, C., Hermwille, L., Kreibich, N., Mersmann, F., Ott, H. E., and Wang-Helmreich, H. (2016). Phoenix from the ashes—an analysis of the Paris agreement to the United Nations framework convention on climate change. *Wuppertal Institute for Climate, Environment and Energy*, 1:1–54.

[Ortega-Vazquez, 2014] Ortega-Vazquez, M. A. (2014). Optimal scheduling of electric vehicle charging and vehicle-to-grid services at household level including battery degradation and price uncertainty. *IET Generation, Transmission & Distribution*, 8(6):1007.

[Pagani et al., 2019] Pagani, M., Korosec, W., Chokani, N., and Abhari, R. S. (2019). User behaviour and electric vehicle charging infrastructure: An agent-based model assessment. *Applied Energy*, 254:113680.

[Pan et al., 2018] Pan, X., Wang, H., Wang, L., and Chen, W. (2018). Decarbonization of China's transportation sector: in light of national mitigation toward the Paris Agreement goals. *Energy*, 155:853–864.

[Pillai and Bak-Jensen, 2010] Pillai, J. R. and Bak-Jensen, B. (2010). Integration of vehicle-to-grid in the western Danish power system. *IEEE transactions on sustainable energy*, 2(1):12–19.

[Proterra, 2021] Proterra (2021). ZX5 Electric Bus. [online] Available at:. https://www.proterra.com/vehicles/zx5-electric-bus/. Accessed June 2021.

[Proterra, 2022] Proterra (2022). Financing Your Electric Bus. [online] Available at:. https://www.proterra.com/services/financing-bus-fleets/. Accessed Jun 2022.

[Ritchie and Roser, 2020] Ritchie, H. and Roser, M. (2020). CO_2 and greenhouse gas emissions. *Our World in Data*. https://ourworldindata.org/co2-and-other-greenhouse-gas-emissions.

[Sadeghianpourhamami et al., 2018] Sadeghianpourhamami, N., Refa, N., Strobbe, M., and Develder, C. (2018). Quantitive analysis of electric vehicle flexibility: A data-driven approach. *International Journal of Electrical Power & Energy Systems*, 95:451–462.

[Santarromana et al., 2020] Santarromana, R., Mendonça, J., and Dias, A. M. (2020). The effectiveness of decarbonizing the passenger transport sector through monetary incentives. *Transportation Research Part A: Policy and Practice*, 138:442–462.

[Sarker et al., 2016] Sarker, M. R., Olsen, D. J., and Ortega-Vazquez, M. A. (2016). Co-optimization of distribution transformer aging and energy arbitrage using electric vehicles. *IEEE Transactions on Smart Grid*, 8(6):2712–2722.

[Sheppard et al., 2016] Sheppard, C. J., Harris, A., and Gopal, A. R. (2016). Cost-effective siting of electric vehicle charging infrastructure with agent-based modeling. *IEEE Transactions on Transportation Electrification*, 2(2):174–189.

[Sofia et al., 2020] Sofia, D., Gioiella, F., Lotrecchiano, N., and Giuliano, A. (2020). Cost-benefit analysis to support decarbonization scenario for 2030: A case study in Italy. *Energy Policy*, 137:111137.

[Spillar, 1997] Spillar, R. J. (1997). Park-and-ride planning and design guidelines.

[Stumpe et al., 2021] Stumpe, M., Rößler, D., Schryen, G., and Kliewer, N. (2021). Study on sensitivity of electric bus systems under simultaneous optimization of charging infrastructure and vehicle schedules. *EURO Journal on Transportation and Logistics*, 10:100049.

[Sustainable-Bus, 2018] Sustainable-Bus (2018). 5 per cent of city buses registered in 2018 in Europe were electric buses. [online] Available at:. https://www.sustainable-bus.com/news/5-per-cent-of-city-buses-registered-in-2018-in-europe-were-electric-buses/. Accessed Jan 2022.

[Sustainable-Bus, 2020] Sustainable-Bus (2020). Electric bus, main fleets and projects around the world. [online] Available at:. https://www.sustainable-bus.com/electric-bus/electric-bus-public-transport-main-fleets-projects-around-world/. Accessed Jan 2022.

[Sweda and Klabjan, 2011] Sweda, T. and Klabjan, D. (2011). An agent-based decision support system for electric vehicle charging infrastructure deployment. In *2011 IEEE Vehicle Power and Propulsion Conference*, pages 1–5. IEEE.

[Tang and Wang, 2022] Tang, H. and Wang, S. (2022). A model-based predictive dispatch strategy for unlocking and optimizing the building energy flexibilities of multiple resources in electricity markets of multiple services. *Applied Energy*, 305:117889.

[Tu et al., 2020] Tu, R., Gai, Y. J., Farooq, B., Posen, D., and Hatzopoulou, M. (2020). Electric vehicle charging optimization to minimize marginal greenhouse gas emissions from power generation. *Applied Energy*, 277:115517.

[U.S. Department of Energy, 2021] U.S. Department of Energy (2021). Alternative Fuels Data Center, U.S. Department of Energy. [online] Available at:. https://afdc.energy.gov/data/10310. Accessed June 2021.

[U.S. Environmental Protection Agency, 2021] U.S. Environmental Protection Agency (2021). Greenhouse gases equivalencies calculator - calculations and references. [online] Available at:. https://www.epa.gov/energy/greenhouse-gases-equivalencies-calculator-calculations-and-references. Accessed June 2021.

[Wei et al., 2018] Wei, R., Liu, X., Ou, Y., and Fayyaz, S. K. (2018). Optimizing the spatio-temporal deployment of battery electric bus system. *Journal of Transport Geography*, 68:160–168.

[Wolbertus et al., 2021] Wolbertus, R., van den Hoed, R., Kroesen, M., and Chorus, C. (2021). Charging infrastructure roll-out strategies for large scale introduction of electric vehicles in urban areas: An agent-based simulation study. *Transportation Research Part A: Policy and Practice*, 148:262–285.

[Xie et al., 2018] Xie, F., Liu, C., Li, S., Lin, Z., and Huang, Y. (2018). Long-term strategic planning of inter-city fast charging infrastructure for battery electric vehicles. *Transportation Research Part E: Logistics and Transportation Review*, 109:261–276.

[Xu et al., 2016] Xu, B., Oudalov, A., Ulbig, A., Andersson, G., and Kirschen, D. S. (2016). Modeling of lithium-ion battery degradation for cell life assessment. *IEEE Transactions on Smart Grid*, 9(2):1131–1140.

[Yang et al., 2017] Yang, J., Dong, J., and Hu, L. (2017). A data-driven optimization-based approach for siting and sizing of electric taxi charging stations. *Transportation Research Part C: Emerging Technologies*, 77:462–477.

[Zhang et al., 2017] Zhang, H., Moura, S. J., Hu, Z., Qi, W., and Song, Y. (2017). A second-order cone programming model for planning PEV fast-charging stations. *IEEE Transactions on Power Systems*, 33(3):2763–2777.

[Zhou, 2022] Zhou, Y. (2022). Light duty electric drive vehicles monthly sales updates. [online] Available at:. https://www.anl.gov/es/light-duty-electric-drive-vehicles-monthly-sales-updates. Accessed Jan 2022.

[Zuo et al., 2020] Zuo, T., Wei, H., and Chen, N. (2020). Promote transit via hardening first-and-last-mile accessibility: Learned from modeling commuters' transit use. *Transportation Research Part D: Transport and Environment*, 86:102446.

Appendices

A Obtaining the Minimal Home Charging Cost $C_j^{EV,min}$

To determine $C_j^{EV,min}$, the minimal cost of home charging for each individual EV j, we solve the following optimization problem (32)-(36):

$$\min \sum_{t\in T} \left(c_t^{e,home} y_{jt} + c^{deg}|y_{jt}| \right) \Delta t, \tag{32}$$

Subject to:

$$e_{jt'}^{v} = e_{jt}^{v} + \left[y_{jt} - (1-\sqrt{\kappa})|y_{jt}| - s_{jt}^{v} \right] \Delta t, \quad \forall t \in T, t' = Next(t) \tag{33}$$

$$e^{v,min} \le e_{jt}^{v} \le e^{v,max}, \quad \forall t \in T, \tag{34}$$

$$0 \le y_{jt} \le y^{home,max}, \quad \forall t \in T_j^{home}, \tag{35}$$

$$y_{jt} = 0, \quad \forall t \notin T_j^{home} \tag{36}$$

Finally, we can obtain $C_j^{EV,min} = D\sum_{t\in T} \left(c_t^{e,home} y_{jt} + c^{deg}|y_{jt}| \right) \Delta t, \forall j \in J.$

B Linearization of Constraints

B.1 Linearization of (22) and (23)

First of all, (22) is equivalent to the following two equations (37) and (38):

$$\hat{x}_{ikt} = \{0,1\}, \qquad \forall i \in I, \forall t \in T \tag{37}$$

$$\left| \frac{\beta_{ikt} x_{it}}{G} \right| \le \hat{x}_{ikt} \le |\beta_{ikt} x_{it} G|, \qquad \forall i \in I, \forall t \in T \tag{38}$$

where G is a large positive number and $G \gg \beta_{ikt} x_{it}$. Then, (38) can be linearized to (39a)-(39e):

$$\begin{aligned}
&\hat{x}_{ikt} \ge \frac{\beta_{ikt} x_{it}}{G}, && \text{(39a)}\\
&\hat{x}_{ikt} \ge -\frac{\beta_{ikt} x_{it}}{G}, && \text{(39b)}\\
&\hat{x}_{ikt} \le \beta_{ikt} x_{it} G + X_{ikt} G^{g}, && \text{(39c)}\\
&\hat{x}_{ikt} \le -\beta_{ikt} x_{it} G + (1 - X_{ikt}) G^{g}, && \text{(39d)}\\
&X_{ikt} = \{0,1\} && \text{(39e)}
\end{aligned}$$

where G^g is also a large positive constant, and $G^g \gg \beta_{ikt} x_{it} G$.

The constraints (37) and (39a)-(39b) work in the following way to ensure (22) is satisfied: 1) When $\beta_{ikt} x_{it} = 0$, (39a) and (39b) both require $\hat{x}_{ikt} \ge 0$. One of (39c) and (39d) will requires $\hat{x}_{ikt} \le 0$, regardless of X_{ikt} is 0 or 1. The combined effect will be $\hat{x}_{ikt} = 0$. 2) When $\beta_{ikt} x_{it} \ne 0$, (39a)-(39e) will force $\hat{x}_{ikt} = 1$. For example, if $\beta_{ikt} x_{it} > 0$, X_{ikt} must be 0 to ensure (39d) is valid. Since (39a) requires $\hat{x}_{ikt} \ge$ a small positive number, the result will be $\hat{x}_{ikt} = 1$. Similar effect can be found with $\beta_{ikt} x_{it} < 0$.

By referencing (37) and (39a)-(39b), we further linearize (23) as shown below:

$$\hat{y}_{jkt} = \{0,1\}, \qquad \forall j \in J, \forall t \in T \tag{40}$$

$$\hat{y}_{jkt} \geq \frac{\gamma_{jkt} y_{jt}}{G}, \tag{41a}$$
$$\hat{y}_{jkt} \geq -\frac{\gamma_{jkt} y_{jt}}{G}, \tag{41b}$$
$$\hat{y}_{jkt} \leq \gamma_{jkt} y_{jt} G + Y_{jkt} G^g, \tag{41c}$$
$$\hat{y}_{jkt} \leq -\gamma_{jkt} y_{jt} G + (1 - Y_{jkt}) G^g, \tag{41d}$$
$$Y_{jkt} = \{0, 1\} \tag{41e}$$

806 **B.2 Linearization of** (24)

807 (24) can be linearized to the following equations:

$$(N_k^b + N_k^v) \geq -G\delta_k + g, \quad \forall k \in K \tag{42a}$$
$$(N_k^b + N_k^v) \leq G(1 - \delta_i), \quad \forall k \in K \tag{42b}$$
$$\hat{N}_k \geq 1 - G\delta_k, \quad \forall k \in K \tag{42c}$$
$$\hat{N}_k \leq 1 + G\delta_k, \quad \forall k \in K \tag{42d}$$
$$\hat{N}_k \geq -G(1 - \delta_k), \quad \forall k \in K \tag{42e}$$
$$\hat{N}_k \leq G(1 - \delta_k), \quad \forall k \in K \tag{42f}$$
$$\delta_k = \{0, 1\}, \qquad \forall k \in K \tag{42g}$$

808 where $g \ll 1$ is a small positive number.

809 The constraints (42a)-(42g) work in the following way to satisfy (24): 1) When the number of chargers is greater than 810 0, i.e. $(N_k^b + N_k^v) > 0$, (42a) and (42b) combined require $\delta_k = 0$, in which case $\hat{N}_k = 1$ as enforced by (42c) and 811 (42d). 2) On the other hand, When the number of chargers is 0, i.e. $(N_k^b + N_k^v) = 0$, (42a) and (42b) combined require 812 $\delta_k = 1$, and in this case, (42e) and (42f) will limit $\hat{N}_k$ to be 0.

Zuzhao Ye: Conceptualization, Methodology, Software, Validation, Formal analysis, Investigation, Resources, Data Curation, Writing - Original Draft, Writing - Review & Editing, Visualization.

Nanpeng Yu: Conceptualization, Methodology, Validation, Formal analysis, Investigation, Resources, Writing - Review & Editing, Supervision, Project administration, Funding acquisition

Ran Wei: Conceptualization, Methodology, Validation, Formal analysis, Investigation, Resources, Writing - Review & Editing, Supervision, Project administration, Funding acquisition.

Xiaoyue Cathy Liu: Conceptualization, Writing - Review & Editing.